

Multi target interactions of essential oil nanoemulsion of *Cinnamomum travancoricum* against diabetes mellitus via *in vitro*, *in vivo* and *in silico* approaches

Venkatraman Sriramavaratharajan^a, David Raj Chellappan^b, Shanmugam Karthi^a, Mathialagan Ilamathi^c, Ramar Murugan^{d,*}

^a School of Chemical and Biotechnology, SASTRA Deemed University, Thanjavur 613 401, Tamil Nadu, India

^b Central Animal Facility, School of Chemical and Biotechnology, SASTRA Deemed University, Thanjavur 613 401, Tamil Nadu, India

^c Institute of Bioorganic Chemistry, Polish Academy of Science, Poznan, Poland

^d Centre for Research and Postgraduate Studies in Botany, Ayya Nadar Janaki Ammal College, Sivakasi 626124, Tamil Nadu, India



ARTICLE INFO

Keywords:

Cinnamomum travancoricum

Wild cinnamon

Essential oil

Nanoemulsion

Antidiabetic

ABSTRACT

This study reports antidiabetic activity of leaf essential oil (EO) of *Cinnamomum travancoricum* from the Western Ghats, India via *in vitro*, *in vivo* and *in silico* methods. EO was characterized by GC-MS and GC-FID. Essential oil nanoemulsions (EN) were prepared and characterized. Antidiabetic potential was evaluated through *in vitro* assays namely, α -amylase and α -glucosidase inhibition, glucose uptake and insulin secretion assays. *In vivo* study was conducted on STZ-induced diabetic Wistar rats. Molecular docking was conducted to find the lead antidiabetic compounds. Of the 42 compounds identified in the EO, α -phellandrene (5.9%), β -phellandrene (12.6%), linalool (23.6%), safrole (6.8%) and shyobunol (5.1%) were major constituents. Of the two ENs formulated, 1:2 ratio (EO to surfactants) was better in zeta size (51.4 nm) and potential (-30.9). *In vitro* results were impressive. EN lowered elevated blood glucose level to normal ($p < 0.01$) and improved the insulin secretion ($p < 0.01$) in diabetic rats. Further, serum AST, ALT, ALP, triglyceride and pancreatic β -cell damage were seen reduced ($p < 0.05$). Molecular docking studies showed minor constituents of EO, namely, δ -cadinen, elemol, spathulenol and α -copaen-11-ol playing active role in antidiabetic activity through α -amylase, α -glucosidase, insulin receptor, and insulin secretion proteins.

1. Introduction

Nature provides a range of cures for the treatment of various diseases. About 80% of the world's human population relies on traditional remedies for their medical needs [1,2]. Traditional medicines use plant extracts or their active ingredients. Many therapeutic plants, herbal formulations and plant-based medications are thought to be safer than synthetic drugs [3]. Although therapeutically active molecules from many medicinal plants are least described, these medicinal plants are still prescribed because of their safety, efficacy, efficiency and accessibility [2,4]. The World Health Organization (WHO) acknowledges that plant-based disease management is effective, safe and has few or no side effects [5]. As a result, WHO encourages the use of herbal remedies to treat a variety of medical conditions, including diabetes [6].

Diabetes mellitus is a metabolic disorder due to chronic

hyperglycemia, which is caused by impaired metabolism of carbohydrates, fats and proteins and relative deficiency of insulin secretion and action [7]. The occurrence of diabetes has drastically increased and it is a major public health problem. About 451 million people have been affected by diabetes since 2017 and it is predicted to rise to 693 million by 2045 [8]. The number of diabetic patients is fast growing at an alarming rate in the world, particularly in Asia, which is the 'epicenter of diabetes' [9]. International Diabetes Federation reports that India has the second highest population of diabetes in the world and is predicted to become the first by 2045 [8]. Pharmacological treatment is designed to control glycemia and to decrease the chances of diabetic complications. Many classes of hypoglycemic drugs with different mechanisms of action have been used to maintain optimal blood glucose level. Insulin sensitizers (Biguanides & Thiazolidinediones), insulin secretagogues (Sulfonylureas & Meglitinide derivatives), α -glucosidase inhibitors,

* Corresponding author.

E-mail address: ramarmurugan@yahoo.com (R. Murugan).

DPP-4 inhibitors and exogenous insulin are widely used to manage diabetes mellitus [10]. However, continued use of these conventional drugs causes many adverse health effects [11]. Therefore, people use traditional medicines to manage diabetes. Further, there is an endless search for safe and cost-effective medicines for diabetes from natural sources [12].

Despite the availability of numerous antidiabetic medications in the pharmaceutical market, medicinal plants are also equally popular [13]. Medicinal plants are the best source for treating diabetes in developing countries, as they are less expensive than synthetic drugs. They contain several phytochemicals such as alkaloids, carotenoids, flavonoids, glycosides, saponins, and terpenoids which have a potential antidiabetic effect [14]. A vast number of plants have been documented to possess antidiabetic activity [15]. More than 1200 plant species have been used in traditional antidiabetic remedies and a majority of these plants are relatively effective [16]. Recent studies report that many medicinal plants such as *Capparis spinosa*, *Juglans regia*, *Brassica oleracea* convar. *botrytis* var. *cymosa* (Broccolo Fiolaro) and *Brassica oleracea* convar. *acephala* var. *sabellica* (Cavolo Nero) and Gum arabic have antidiabetic activities [17–20]. Further, the chemical compounds found in many therapeutically potential medicinal plants could be used as lead molecules in the development of bioactive components [2].

Cinnamomum Schaeffer belonging to Lauraceae family is an economically and medicinally valuable genus. This genus is distributed in tropical and subtropical Asia-Pacific and South America. It is represented by about 250 species globally, of which 45 species are distributed in India [21]. The Western Ghats in India is the center of origin of some important spices including black pepper, cardamom and cinnamon. This mega biodiversity region holds 21 wild *Cinnamomum* species [22], of which 16 are endemic. Globally, the name cinnamon refers to *Cinnamomum verum*, a popular spice and a medicinal plant since time immemorial, which is used in antidiabetic formulations [23]. Apart from being used as a spice, the leaf and bark of cinnamon have been used in different traditional systems of medicine. Cinnamaldehyde, the main constituent of bark essential oil of cinnamon, is reported to have antidiabetic property [24]. Further, methylhydroxychalcone, polyphenol Type-A polymers and naphalenemethyl ester of 3,4-dihydroxycinnamic acid from cinnamon are reported to have insulin mimicking and antidiabetic properties respectively [25–27]. Apart from these isolated molecules from cinnamon species, extracts from other commercially important cinnamon species, namely, *C. cassia* and *C. tamala* and a few wild species, namely, *C. bejolghota*, *C. loureirii*, and *C. osmophloeum* have also been reported to possess antidiabetic activities [28,29]. Recently, a few wild *Cinnamomum* species, namely, *C. chemungianum*, *C. litseifolium*, *C. walaiwarense*, and *C. wightii* have been investigated by us for their antidiabetic potential [30–33].

Cinnamomum travancoricum Gamble (CT) is an endemic species distributed in the Agasthyamalai region of southern Western Ghats. The bark of CT is used to treat asthma, backache, cough, cold, dental diseases, mouth diseases, thirst, vomiting, stomach pain, wounds, and urinary problems [34,35]. The bark of CT is reported to contain anthraquinones, cardiotonic glycosides, cyanogenic glycosides, leucoanthocyanins, saponins, steroids, triterpenes, essential oils, fixed oils, saponins, sugar, tannins, and triterpenoids, whereas leaf contains camphor as a major compound [35–38]. The bark extract of CT is reported to have hepatoprotective activity [35]. Since CT possesses various biological activities, the present study aimed to evaluate its antidiabetic activity via *in vitro*, *in vivo*, and *in silico* approaches.

2. Materials and methods

2.1. Sample collection and preparation

Mature leaves of CT were collected in March 2017 from Agasthyamalai hills (Latitude 8.62051; Longitude 77.24901), southern Western Ghats, India. Herbarium specimens (*R. Murugan 175*) were prepared and

deposited at the Herbarium of Ayya Nadar Janaki Ammal College, Sivakasi, India. The collected samples were identified by an Angiosperm Taxonomist (the corresponding author) and further confirmed by matching the specimens with authentic herbarium specimens (K000778623, K000778624) deposited at Royal Botanic Gardens, Kew, London.

2.2. Extraction and characterization of EO

Extraction of essential oil (EO) of CT was carried out by the methods previously followed by us [39]. After collection, the leaves were dried in shade for two weeks. The shade dried leaves were hydro-distilled at 100 °C initially for 30 min and reduced to 60 °C for 5 h to extract the EO. Qualitative and quantitative analyses of the EO were carried out by Gas Chromatography-Mass Spectrometry (GC-MS) and Gas Chromatography-Flame Ionization Detector (GC-FID) respectively.

2.2.1. Qualitative analysis with GC-MS

GC-MS analysis was performed using PerkinElmer Clarus 500 Gas Chromatograph fitted with Elite-5MS, non-polar, capillary column (30 m × 0.25 mm × 250 µm) coated by 5% phenyl 95% dimethyl polysiloxane. Turbo Mass Gold Quadrupole Mass Spectrometer was used. The initial temperature of the oven was 60 °C and increased to 240 °C at the pace of 3 °C/min with a final holding time of 5 min. The injector temperature was maintained at 270 °C. Helium was used as carrier gas at the flow rate of 1 mL/min. One µL of EO dissolved in hexane was injected and its split ratio was 1:20. In the electron ionization (EI) mode, mass spectra with ionization energy of 70 eV and a scan range of 40–600 amu were recorded. The ion source and transfer line temperatures were maintained at 180 °C and 200 °C respectively.

2.2.2. Quantitative analysis with GC-FID

GC-FID analysis was performed using Agilent 7890 B Gas Chromatograph fitted with non-polar, capillary, Elite-5MS, non-polar, capillary column (30 m × 0.25 mm × 250 µm) coated by 5% phenyl 95% dimethyl polysiloxane and attached to Flame Ionization Detector (FID). The initial temperature of the oven was 60 °C and increased to 240 °C at the rate of 3 °C/min. The injector and detector temperature was held at 250 °C. Helium was used as carrier gas at the flow rate of 1 mL/min. One µL of EO dissolved in hexane was injected and the split ratio was 1:10. Standard *n*-alkanes (C₈ to C₂₀) (Sigma Aldrich) were also run similar to that of EO sample in the same condition for calculating retention index (RI) value of each of the chemical compounds present in the EO. The RI value of each compound was calculated. The compounds were identified by comparing RI value and mass spectra of the components present in the EO with that of the standard spectra and RI values available in the literature [40] and NIST 2005 MS library. Quantification of each component of the EO was done from FID peak area percentage without the use of internal standard of correction factors.

2.3. Preparation and characterization of EO nanoemulsions

Essential oil nanoemulsion (EN) of CT was prepared by high shear stirring technique using high speed homogenizer followed by ultrasonication. Two sets of EN (1:1 and 1:2 ratio of EO to surfactants) were prepared. The 1:1 ratio of EN was formulated by mixing 1% surfactants [0.5% tween 80 (HiMedia, India), 0.25% propylene glycol (HiMedia, India) & 0.25% soya lecithin (HiMedia, India)] with 1% EO (w/v) and 98% distilled water. The 1:2 ratio EN was prepared by mixing 2% surfactants (1% tween 80, 0.5% propylene glycol & 0.5% soya lecithin) with 1% EO (w/v) and 97% distilled water. Initially, the coarse emulsion was prepared by consecutively mixing the EO with tween 80, propylene glycol and soya lecithin (dissolved in water). Then the coarse emulsion was subjected to homogenization at 8000 rpm for 10 min (REMI, India). Further it was subjected to ultrasonication for 10 min (with 30 s pulse on and 30 s off) using a 6 mm probe at 50 kHz and power output of 250 W

probe sonicator (PRO-250, Labman, India). The heat generation during the homogenization and ultrasonication was reduced by keeping the emulsions on an ice bath.

The hydrodynamic average size, zeta potential and polydispersity index (PDI) of the EN of CT were measured via Dynamic Light Scattering method using particle size analyzer (Zeta Sizer Nano Zs, ZEN3600, Malvern Instruments, UK). The EN was 20 times diluted with deionized water to avoid multiple scattering effects. The morphology and size of the selected EN of CT (based on the size and potential), which was chosen for further studies, were analyzed by transmission electron microscope (TEM). For TEM analysis, a drop of EN on a 200-mesh carbon-coated copper grid (Electron Microscopy Sciences) was placed and dried under vacuum. The EN was negatively stained using 2% ammonium molybdate (w/v), and again dried under vacuum. The size and morphology of the EN of CT were observed via TEM (JEOL-JEM 1011) at a magnification of 40,000 x at an acceleration voltage of 200 KV. After characterization, the EN of CT was stored under refrigeration and further used for *in vitro* and *in vivo* studies.

2.4. *In vitro* assays

2.4.1. *In vitro* enzymatic assays

α -Amylase and α -glucosidase inhibitory assays were carried out as per methods of Sriramavaratharajan & Murugan [30].

2.4.2. *In vitro* cell line based assays

2.4.2.1. Cell culture maintenance. Rat skeletal myoblast cells (L6) and mouse insulinoma pancreatic β -cells (MIN6) were acquired from National Center for Cell Science, Pune, India. L6 cells were grown in DMEM medium (having 10% FBS) (HiMedia, India) whereas MIN6 cells were grown in DMEM high glucose medium (supplemented with heat-inactivated serum at 15% concentration) (HiMedia, India) and cultured at 37 °C with 5% CO₂ at pH 7.4.

2.4.2.2. Cytotoxic assay. 3-(4,5-dimethylthiazol-2-yl)-2,5-diphenyltetrazolium bromide (MTT) assay was performed to find out the nontoxic dose of EN of CT [41]. After reaching 70% confluence, 4000–6000 cells / well were cultured in a 96-well plate. Then different concentrations of EN (100, 50, 25, 12.5, and 6.25 μ g/mL) were added. The experiment was performed in triplicates with cells containing vehicle control (VC) (without EO but the same volume of surfactants). After 24 h treatment, the medium was removed and 20 μ L of MTT (Sigma Aldrich) solution (5 mg/mL in phosphate buffer) and 200 μ L of fresh medium were added, subsequently incubated for 4 h at 37 °C. Then, the medium along with MTT solution was removed and 100 μ L of DMSO (HiMedia, India) was added. Finally, absorbance was measured at 560 nm. Cytotoxicity of the EN for both MIN6 and L6 cell lines was calculated and expressed on percentage basis.

2.4.2.3. Glucose stimulated insulin secretion assay on MIN6 cell line. Glucose stimulated-insulin secretion activity of the EN of CT was assessed according to Sha, Shi, Niu, & Chen [42] with slight modification. Serum-free DMEM medium with 25 mM HEPES (pH 7.4) (HiMedia, India), 2 mM L-glutamine (HiMedia, India) and without glucose was used. Initially, MIN6 cells were cultured on a 96-well plate at a density of 7×10^3 cells/well. The basal medium was prepared using glucose (1 mM) and warmed to 37 °C before use. Cells were washed two times using Krebs-Ringer Bicarbonate buffer (Thermo Scientific) and seeded in a basal serum-free medium for 2 h. Then, the medium was removed and again the cells were incubated using medium consisting of a high concentration of glucose (5 mM) and EN of CT (12.5, 6.25 and 3.125 μ g/mL), standard drug glibenclamide (Himedia, India) (12.5 μ g/mL) and VC for 15 min. After incubation, the cells were lysed by acid/ethanol for the measurement of total insulin content with ELISA kit (Merck).

2.4.2.4. Glucose uptake assay on L6 cell line. Glucose uptake activity of the EN of CT was evaluated as per the method of Kozma et al. [43] with slight modification. Around 4000–6000 L6 cells were cultured on a 96-well plate. Initially, 200 μ L of medium consisting of three different concentrations of EN (25, 12.5 and 6.25 μ g/mL) was added to the differentiated L6 cells and incubated at 37 °C for 48 h. Then, the cells were washed twice in phosphate buffer and incubated with 100 μ L of phosphate buffer consisting of 200 nM insulin (Sigma Aldrich) at 37 °C for 30 min. A separate well is treated with cytochalasin-B (Sigma Aldrich) (without treating insulin) was used as a negative control. After incubation, the cells were washed with phosphate buffer and once again incubated in 100 μ L of phosphate buffer consisting of 2 mM tritium (Thermo Scientific) labeled 2-deoxy glucose (Sigma Aldrich) at a concentration of 1 μ Ci/mL for 30 min at 37 °C. After the incubation, the wells were washed thrice with ice-cold phosphate buffer and lysed with phosphate buffer containing 1% sodium dodecyl sulfate (Sigma Aldrich). Finally, all the treated wells were added with 50 μ L of scintillation cocktail (Sigma Aldrich) for counting the radiation and subsequently, measured the glucose uptake by cells using a liquid scintillation counter (PerkinElmer). Metformin (Himedia, India) (25 μ g/mL) was used as standard drug.

2.5. *In vivo* study

2.5.1. Experimental animals and housing conditions

Healthy Wistar rats (8–12 weeks old) were obtained from the Central Animal Facility, SASTRA Deemed University, Thanjavur, India. The experimental rats were maintained in the following conditions; temperature 22 ± 2 °C, relative humidity 50–56% and a 12 h light and 12 h dark cycle. They were fed with standard rodent pellets (Altromin, Germany) and reverse osmosis water *ad libitum*. Animal experiments were performed as per the guidelines of Committee for the Purpose of Control and Supervision of Experiments on Animals (CPCSEA), India, after approval from the Institutional Animal Ethics Committee (IAEC approval Nos.: 441/SASTRA/IAEC/RPP and 478/SASTRA/IAEC/RPP).

2.5.2. Acute oral toxicity study

As per OECD 425 guidelines, the up and down procedure was followed for the acute oral toxicity study [44]. The study was performed using 10 weeks old female Wistar rats. Before treatment, animals were fasted overnight and after treatment with VC and EN, the feed was made available *ad libitum*. The EN and VC were administered by oral gavage. The rats were grouped into two groups (5 rats in each group); Group I – VC (2% surfactants) and Group II – EN. Symptoms of any toxic effect were monitored during the study period. End of the 14th day, all the rats were euthanized and subjected to necropsy. The organs were macroscopically inspected by a veterinary pathologist for any test substance related toxicity injuries.

2.5.3. Dose optimization study

The study was performed using 8–10 weeks old (weighing between 230 and 280 g) healthy male Wistar rats. Rats were randomly divided into 6 groups of 3 animals in each group. The blood sample was collected from the tail vein 30 min before the oral administration of EN (100, 50, 25, 12.5 and 6.25 mg/kg b.wt.), VC (2% surfactants) and standard drug glibenclamide (5 mg/kg b.wt.). After 30 min, the fasting rats were intraperitoneally administered with 50% D-glucose (Sigma Aldrich) (2 g/kg b.wt.). Blood glucose level was measured (Glucometer, AP Plus) before administration of glucose (0 min) and 30, 60 and 120 min intervals after glucose administration.

2.5.4. Experimental design of Streptozotocin (STZ) induced diabetic study

Diabetes was induced by intraperitoneal injection of STZ (Sigma Aldrich) (35 mg/kg b.wt.) in ice-cold citrate buffer (0.1 M, pH 4.5) after 18 h of fasting. After 72 h, blood glucose level was measured and rats with greater than 250 mg/dL were used for the study. A booster dose of

STZ (30 mg/kg b.wt.) was given to those animals with lesser than less than 250 mg/dL blood glucose. The diabetic rats were randomly grouped into 7 groups (6 rats in each group), namely, normal control (NC) - rats fed with distilled water, diseased control (DC) - rats fed with distilled water, vehicle control (VC) - rats fed with 2% surfactants, standard control (STD) - rats fed with glibenclamide (5 mg/kg b.wt.), low dose (Low) - rats fed with EN (6.25 mg/kg b.wt.), intermediate dose (Medium) - rats fed with EN (12.5 mg/kg b.wt.) and high dose (High) - rats fed with EN (25 mg/kg b.wt.).

After grouping, the animals were orally administered with vehicle, glibenclamide and EN in low, intermediate and high doses for 28 days. Feed intake, weekly body weight and blood glucose level (0, 14 and 28th day) were measured. Intraperitoneal glucose tolerance test (ipGTT) was conducted on 22nd day according to El Kabbaoui et al. [45] with slight modifications. After overnight fasting, all animals were injected with 50% D-glucose (2 g/kg b.wt.) intraperitoneally after 60 min of drug administration. Blood glucose level was measured before (0 min) and after administration of glucose (30, 60 and 120 min).

Blood samples were collected from retro-orbital plexus under mild anesthesia on 28th day. Both plasma and serum were separated from the blood. Serum biochemical parameters, namely, alkaline phosphatase (ALP), alanine amino transferase (ALT), aspartate amino transferase (AST), low-density lipoproteins (LDL), high-density lipoproteins (HDL), total cholesterol (TC) and triglycerides were measured using A15 automated biochemical analyzer with the Biosystems kit. Plasma insulin was estimated using ELISA kit (Diagnostic Products Corporation, The United Kingdom).

Finally, all the animals were euthanized by CO₂ inhalation and pancreas were collected and fixed in neutral buffered formalin (10%). Then the histological examination was carried out to evaluate the pancreatic damages caused by hyperglycemia. Histological assessment of pancreatic tissues was done by fixation, followed by paraffin embedding. About 5 µm cross sections were taken for processing with hematoxylin and eosin staining. After staining, the sections were observed under a Nikon Eclipse Ci trinocular light microscope at a magnification of 10X.

2.6. In silico investigation

2.6.1. Structure of ligands

The structure of the profiled compounds of EO of CT was retrieved from PubChem database (<https://pubchem.ncbi.nlm.nih.gov/>).

2.6.2. Structure of Proteins

The 3D structure of α-amylase (1HNY), α-glucosidase (2ZEO), insulin receptor (1IR3) and Glucagon-like peptide-1 (2ZGM) were retrieved from the protein data bank (PDB) (<http://www.rcsb.org>). All the four target protein structures were prepared using Schrödinger protein preparation wizard (Schrödinger Release 2020–1: Protein Preparation Wizard; Epik, Schrödinger, LLC, New York, NY, 2016; Impact, Schrödinger, LLC, New York, NY, 2016; Prime, Schrödinger, LLC, New York, NY, 2018). Protein preparation briefly includes adding missing hydrogen atoms, correcting metal ionization states to ensure proper formal charge, enumerating bond orders to HET groups, removing co-crystallized water molecules, determining optimal protonation states for histidine residues, optimizing protein's hydrogen bond network, and performing restrained minimization. After restrained minimization, proteins were subjected for quality check and used further for molecular docking studies.

2.6.3. Ligand preparation

The 42 ligands profiled from the chemical composition of CT were prepared for docking using LigPrep (LigPrep, Schrödinger, LLC, New York, NY, 2014). LigPrep generates accurate energy minimized 3D molecular structures to reduce downstream computational errors. It also generates tautomeric states, ionization states, ring conformations, and

stereoisomers for the input structures.

2.6.4. Molecular docking

Schrödinger Glide (Schrödinger Release 2018–1: Glide, Schrödinger, LLC, New York, NY, 2020) program was used for molecular docking. Glide algorithm executes a series of hierarchical searches in the binding region of the receptor and examines all possible binding poses for the input ligand set. Receptor grid was generated using receptor grid generation wizard in Schrödinger. A 3D grid box of size 40 Å × 40 Å × 40 Å was made and kept the center on the binding pocket covering all the essential binding site amino acids. During docking simulation, ligands and active site amino acid residues of proteins were allowed to undergo a conformational change which optimizes the ligand-receptor interaction. While conformational search, to eliminate the unfavorable torsions and high energy conformations, Glide employs a heuristic screening filter. The series of hierarchical filters implemented in Glide algorithm results in high accuracy of prediction of ligand binding modes. During the initial phase of docking calculation, 2000 poses per ligand were generated, out of which best 500 poses per ligand was chosen for further energy minimization. Based on the Glide score function and Glide model energy score, the best-docked structures and their poses were chosen.

2.6.5. MM-GB/SA analysis

After performing Glide docking, MM-GB/SA (Molecular mechanics-generalized- Born/surface area) was performed using Prime module (Prime, Schrödinger, LLC, New York, NY, 2011). This MM-GB/SA predicts the most accurate binding free energy of the protein-ligand complexes. Here the pose viewer file got from molecular docking by Glide algorithm was given as input. OPLS-AA (2005) force field was used for minimizing the energy of the docked pose. Further, the ligand-protein complex energy was computed using generalized-Born/surface area. The binding interactions of the complexes with the lowest binding energies were visualized using the molecular visualization software UCSF Chimera (<https://www.cgl.ucsf.edu/chimera/>) and PyMOL (www.pymol.org).

2.7. Statistical analysis

All the *in vitro* assays were performed in triplicate. Results were shown as mean ± SD. Data were analyzed using either one-way analysis of variance or two-way analysis of variance followed by Tukey multiple comparison tests (GraphPad Prism 6 software, GraphPad Software Inc., USA). *P* values of < 0.05 were recognized as statistically significant.

3. Results and discussion

3.1. Chemical characterization of EO

The shade dried leaves of CT yielded 0.6% v/w EO on hydro-distillation. On GC-FID and GC-MS analyses, 42 chemical compounds amounting to 99.9% of the EO were identified (Table 1). Linalool (23.6%), β-phellandrene (12.6%), safrole (6.8%), α-phellandrene (5.9%) and shyobunol (5.1%) were the major constituents.

CT is a wild aromatic plant which has been proven to possess various medicinal properties, except that of being antidiabetic [46]. Therefore, the present study was conceptualized to investigate antidiabetic effect of the leaf EO of CT via *in vitro*, *in vivo* and *in silico* methods. As a first step, the chemical characterization of leaf EO of CT was done by GC-MS and GC-FID analyses. In a recent study, the leaf EO of CT collected from Munnar region of the Western Ghats was reported to contain α-terpinene (14.5%) and (Z)-β-ocimene (31.1%) as the major constituents [47]. But in the present study, these two compounds were not identified as major components, though α-terpinene (4.1%) is seen as a minor compound. α-Phellandrene (2.0%) and linalool (2.5%) reported as minor components in the previous study, were the major compounds in the present investigation. The difference in chemical composition of EOs of CT from

Table 1
Chemical composition of the leaf EO of *C. travancoricum*.

S.No.	RI ^{Cal}	RI ^{Lit}	Constituents	CAS No.	Area %
1	928	930	α-Thujene	2867-05-2	1.2
2	936	939	α-Pinene	80-56-8	3.9
3	953	954	Camphene	79-92-5	0.8
4	973	975	Sabinene	3387-41-5	2.2
5	977	979	β-Pinene	127-91-3	2.4
6	989	990	Myrcene	123-35-3	1.2
7	999	1002	α-Phellandrene	99-83-2	5.9
8	1014	1017	α-Terpinene	99-86-5	4.1
9	1025	1029	β-Phellandrene	555-10-2	12.6
10	1049	1050	β-(E)-Ocimene	3779-61-1	1.5
11	1058	1059	γ-Terpinene	99-85-4	0.3
12	1088	1088	Terpinolene	586-62-9	0.1
13	1092	1096	Linalool	78-70-6	23.6
14	1120	1121	cis-p-Mentha-2-en-1-ol	29803-82-5	0.1
15	1175	1177	Terpinen-4-ol	562-74-3	0.2
16	1183	1185	Cryptone	500-02-7	0.6
17	1187	1188	α-Terpineol	98-55-5	0.4
18	1205	1208	trans-Piperitol	16721-39-4	0.5
19	1251	1252	Piperitone	89-81-6	0.1
20	1283	1287	Safrole	94-59-7	6.8
21	1336	1338	δ-Elemene	20307-84-0	0.3
22	1346	1349	α-Terpinyl acetate	80-26-2	2.2
23	1371	1373	α-Ylangene	14912-44-8	1.1
24	1388	1390	β-Elemene	515-13-9	2.4
25	1418	1419	(E)-Caryophyllene	87-44-5	0.5
26	1438	1439	α-Guaiene	3691-12-1	0.2
27	1453	1454	α-Humulene	6753-98-6	0.4
28	1457	1460	allo-Aromadendrene	25246-27-9	3.7
29	1497	1500	Bicyclogermacrene	24703-35-3	2.6
30	1507	1509	Germacrene A	28387-44-2	0.2
31	1511	1513	γ-Cadinene	39029-41-9	0.2
32	1521	1523	δ-Cadinene	483-76-1	0.4
33	1532	1534	trans-Cadin-1,4-diene	38758-02-0	0.6
34	1538	1541	α-Copaen-11-ol	41370-56-3	2.4
35	1547	1549	Elemol	639-99-6	0.5
36	1573	1575	Germacrene D-4-ol	198991-79-6	1.0
37	1576	1578	Spathulenol	6750-60-3	0.2
38	1588	1590	Globulol	51371-47-2	0.3
39	1625	1628	1-epi-Cubenol	19912-67-5	2.9
40	1642	1646	α-Muurolol	19435-97-3	4.1
41	1652	1654	α-Cadinol	481-34-5	0.1
42	1684	1689	Shyobunol	35727-45-8	5.1
Total				99.9	

RICal – Retention index value calculated on HP-5 capillary, non-polar column;
RILit – Retention index value in literature [19].

two far away locations (Agasthyamalai and Munnar) might be due to varied ecological conditions. Further, camphor (80%) is also reported as a major compound in CT [48].

3.2. Characterization of EN of CT

Hydrodynamic average size, PDI and zeta potential values of EN of CT are listed in Table 2. Of the two sets of EN, 1:2 EO to surfactants ratio exhibited a droplet size of less than 200 nm for up to 60 days duration that is within the acceptance range of 20–200 nm [49].

Table 2
Hydrodynamic average size, Polydispersity index and Zeta potential values of the EN.

S. No.	Parameters	1:1		1:2	
		1 st day	60 th day	1 st day	60 th day
1	Droplet size (nm)	98.6 ± 1.24	255.7 ± 2.16	51.4 ± 0.80	131.9 ± 1.57
2	Polydispersity Index value	0.649 ± 0.008	0.688 ± 0.007	0.236 ± 0.005	0.255 ± 0.005
3	Zeta potential	-12.5 ± 0.72	-7.08 ± 0.43	-30.9 ± 0.46	-20.6 ± 1.57

Values are mean ± S.D (n = 3).

PDI value defines the homogenous or heterogeneous nature of droplet size distribution in the nanoemulsion. PDI values under 0.2 indicate monodispersity (homogenous suspension), whereas the value nearby 1 indicates polydispersity (heterogeneous suspension) [50]. In the present study, of the two sets of EN, 1:1 ratio was polydispersed whereas the 1:2 ratio was monodispersed (Table 2). Zeta potential can contribute to nanoemulsion stability as surface charge of the particles can keep the stability of formulations for a longer time through electrostatic repulsion and inhibiting destabilization processes like droplets coalescence and Ostwald ripening [51]. Zeta potential value greater than 30 mV with either positively or negatively charged particles are considered as a stable nanoemulsion [52]. It was found that 1:2 ratio EN had superior stability than 1:1 ratio in terms of zeta potential (Table 2).

Based on the above findings, it was found that 1:2 ratio EN was better than the 1:1 ratio. Therefore, 1:2 ratio EN was used for further studies and characterized using TEM. The morphology and size of the 1:2 ratio EN are shown in Fig. 1. Spherical morphology with an average droplet size of 22.29 nm was observed which was interrelated to the average droplet size 51.4 nm recorded using particle size analyzer.

The hydrophobic nature of the EOs makes the delivery of the drug targets problematic. One of the soundest ways to counteract this issue is formulating the extracts/compounds in nanostructured forms, which can enhance the bioavailability, stability, solubility and bio-distribution [53]. Currently, nano-based delivery methods play a lead role to meliorate the efficacy of herbal extracts in the treatment of various diseases [54]. Nanoformulations of herbal extracts such as solid lipid nanoparticles, nanostructured lipid carriers and nanoemulsions colloidal systems remarkably increase the antidiabetic activity of the extracts when matched with conventional formulations. Moreover, the high stability nanoemulsion can be a better choice to deliver the hydrophobic extracts to mend bioavailability and reduce the required dose [54].

Nanoemulsions are colloidal dispersions composed of two immiscible liquids blended using a surfactant with 20–200 nm diameter of droplet size [51]. In the present study, nanoemulsion prepared with 1:2 EO to surfactant ratio was in nano range for up to 60 days of preparation. Generally, the surfactant determines the size and stability of the nanoemulsion droplets [55]. Mostly, the high amount of surfactant to oil ratio decreases the diameter of the droplets [56]. The present study also corroborates the same. Further, increasing the duration of ultrasonication could reduce the droplet size of nanoemulsion [57]. However, an extended period of sonication could generate heat, which would

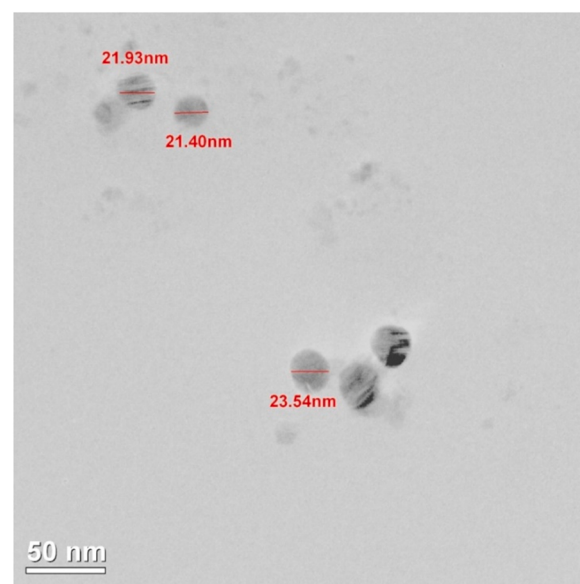


Fig. 1. TEM image of the EN of *C. travancoricum*.

damage the volatile components of EO [58].

The selection of surfactants is crucial in the preparation of nano-emulsions. Non-ionic surfactants are preferable as they are generally regarded as safe and biocompatible and also less affected by pH and alterations in ionic strength. Further, hydrophilic-lipophilic balance (HLB) of the surfactants is vital for oil-in-water nanoemulsion and HLB should be greater than 10 [59]. The combination of surfactant and emulsifier could improve the formation and stability of the oil in water nanoemulsion [60]. Therefore, a mixture of surfactants was used in the present study. Tween 80 was used as a surfactant which has HLB value of 15 and is also a small molecule surfactant that potentially reduces the droplet size. Propylene glycol was used as a co-surfactant, as it facilitates the nano-dispersion formation and alters the surfactant, which reduces the size of the nanoemulsion [61]. Soya lecithin was used as an emulsifier, as it contributes to repulsive electrostatic interactions and thus increases the stability of emulsions [61]. Soy lecithin also greatly interacts with cellular membranes thereby improving absorption of bioactive components [62].

3.3. α -Amylase and α -glucosidase inhibitory activities

The EN of CT inhibited both α -amylase and α -glucosidase enzymes with IC_{50} value of 4.652 ± 0.093 and 3.407 ± 0.040 mg/mL respectively (Fig. 2). However, it was comparably less than the standard drug, acarbose (Sigma Aldrich) ($IC_{50} 7.2 \pm 0.31$ µg/mL). Earlier, leaf EOs of *C. chemungianum*, *C. litseifolium*, *C. walaiwarense* and *C. wightii* from the Western Ghats were evaluated for α -amylase and α -glucosidase inhibitory activities [30–33]. Among these, *C. chemungianum* exhibited excellent α -amylase and α -glucosidase inhibitory activities [30].

Initially, *in vitro* α -amylase and α -glucosidase inhibitory assays were performed to evaluate the antidiabetic effect of the EN of CT. α -Amylase is involved in the hydrolysis of starch and α -Glucosidase is involved in the conversion of disaccharides into glucose. Inhibition of these enzymes can control the postprandial blood glucose level. The outcome of the present study revealed EN of CT exhibited moderate inhibition of both enzymes when compared to the positive control, acarbose. However, the moderate activity of these two enzymes is recommended in diabetic condition so as to avoid the development of flatulence and diarrhea triggered by the fermentation of undigested carbohydrates by unbalanced bacterial activities [63]. Therefore the mild inhibitory activity of α -amylase and α -glucosidase of EN of CT is ideal for the treatment of diabetes.

3.4. Cell toxicity study

Dose optimization of the EN of CT for both MIN6 and L6 cell lines was evaluated by MTT cell proliferation assay. The EN at the

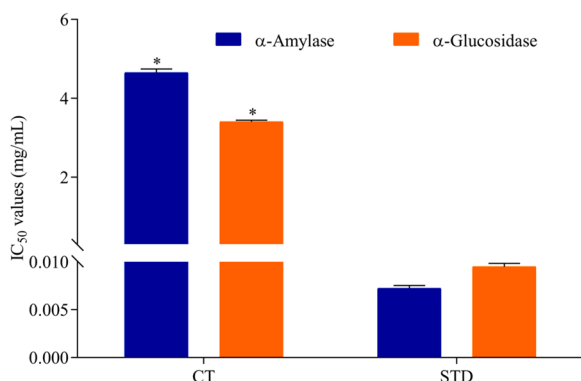


Fig. 2. Effect of the EN of *C. travancoricum* on α -amylase and α -glucosidase inhibitory activities. Values are mean \pm S.D (n = 3); CT – EN of *C. travancoricum*; STD – acarbose. * $P < 0.01$ vs STD.

concentration of 12.5 and 25 µg/mL showed no toxic effect for MIN6 and L6 cells respectively (Fig. 3a & b). Therefore, from these two concentrations of EN, further insulin secretion and glucose uptake assays were carried out.

3.5. Glucose stimulated insulin secretion activity

The nontoxic (> 95% viability) concentration of EN of CT (12.5 µg/mL, 6.25 µg/mL and 3.125 µg/mL), VC and positive control, glibenclamide (12.5 µg/mL) were used for the study (Fig. 4a). No insulin secretion was detected in VC. However, EN improved glucose-stimulated insulin secretion in MIN6 cells based on its concentration. The EN at 12.5 µg/mL exhibited maximum insulin secretion of 1.61 fold \pm 0.05 than the VC, whereas glibenclamide increased the insulin secretion 2.36 fold \pm 0.03 than the VC (Fig. 4a).

Glucose-stimulated insulin secretion assay using MIN6 cells was carried out since defective or insufficient insulin secretion is the major problem in both Type 1 and Type 2 diabetes. When glucose enters into the β cells, the insulin secretion pathway is initiated. As soon as glucose is metabolized through glycolysis and oxidative phosphorylation, the ATP:ADP ratio is increased, which causes ATP-dependent K^+ channels (K ATP) closure and depolarization of plasma membrane [64–67]. This progress directs the opening of voltage-gated calcium channels, permitting Ca^{2+} to get into the cells, leading to insulin exocytosis [68]. Further, the shutting of the K ATP channel facilitates the amplifying effects of glucose and other secretagogues, such as incretins GLP-1 and GIP [69]. In the present study, the glucose stimulated-insulin secretion effect of the EN of CT might be enabled by either directly closing the K^+ channels (KATP) or indirectly stimulating the incretin hormone GLP-1 which in turn work as insulin secretagogues in response to glucose.

3.6. Glucose uptake activity

The nontoxic (> 95% viability) concentration of the EN of CT (25 µg/mL, 12.5 µg/mL and 6.25 µg/mL), VC and positive control, metformin (25 µg/mL) were used for the study (Fig. 4b). No glucose uptake was observed in VC. However, the EN enhanced the glucose uptake in L6 cells in dose dependent manner. Maximum glucose uptake activity (1.15 \pm 0.11 fold vs. VC) was observed at 25 µg/mL concentration. Although the EN of CT showed glucose uptake, it was significantly ($P < 0.01$) lower than metformin (1.67 \pm 0.04 fold vs. control) (Fig. 4b).

Insulin resistance is a major problem for people with type 2 diabetes. The skeletal muscle is involved in 80% of insulin-stimulated glucose uptake in postprandial state and thus, plays a crucial role in managing glucose homeostasis [70]. Type 2 diabetes people predominantly have decreased insulin-regulated glucose uptake [71]. Improving glucose uptake reduces insulin resistance thereby effectively treating diabetes. Insulin regulates the glucose uptake by binding with insulin receptor proteins which are on cell surface, stimulating a sequence of actions that are followed by the translocation of GLUT-4 protein to the cell surface [72]. Because of insulin resistance, the cells involve in imperfect translocation of GLUT-4 to the cell surface, which results in reduced insulin-stimulated glucose transport [73]. Therefore improving the glucose uptake by the activation of GLUT-4 translocation could lead to enhancing insulin sensitivity [74]. In the present study, EN of CT treated along with insulin shows effective glucose uptake which might be due to the insulin-mimetic property of EN that helps in binding with the insulin receptor thereby further activating GLUT-4 translocation.

3.7. Effect of EN on acute oral toxicity

In acute oral toxicity study, both VC and EN of CT up to 2000 mg/kg b.wt. showed no mortality. However, on administration of 2000 mg/kg b.wt. of EN, salivation was observed for the first 1 h. But, administration of 550 mg/kg b.wt. of EN exhibited no toxic effects or salivation. Further, no noticeable gross pathology was observed on 14th day.

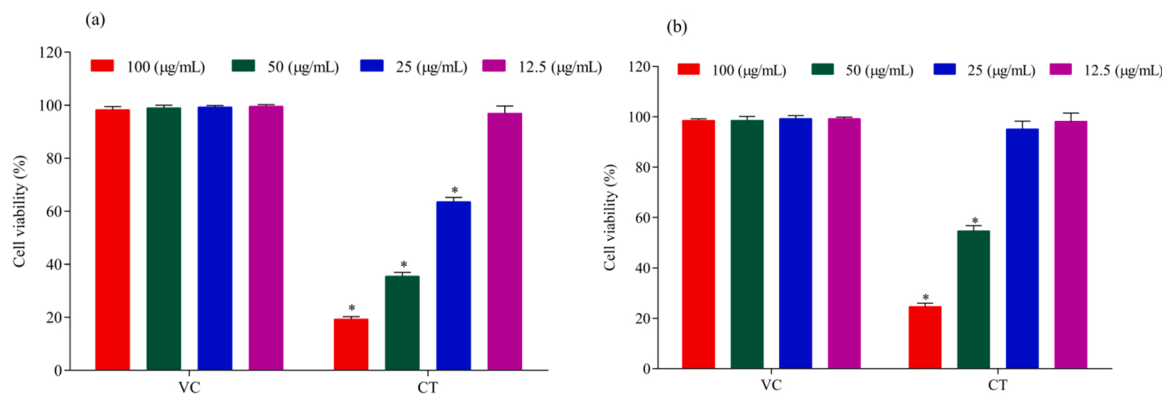


Fig. 3. Cytotoxic effect of the EN of *C. travancoricum* on (a) MIN6 and (b) L6 cell lines. Values are mean \pm S.D (n = 3); VC – vehicle control; CT – EN of *C. travancoricum*. *P < 0.01 vs VC.

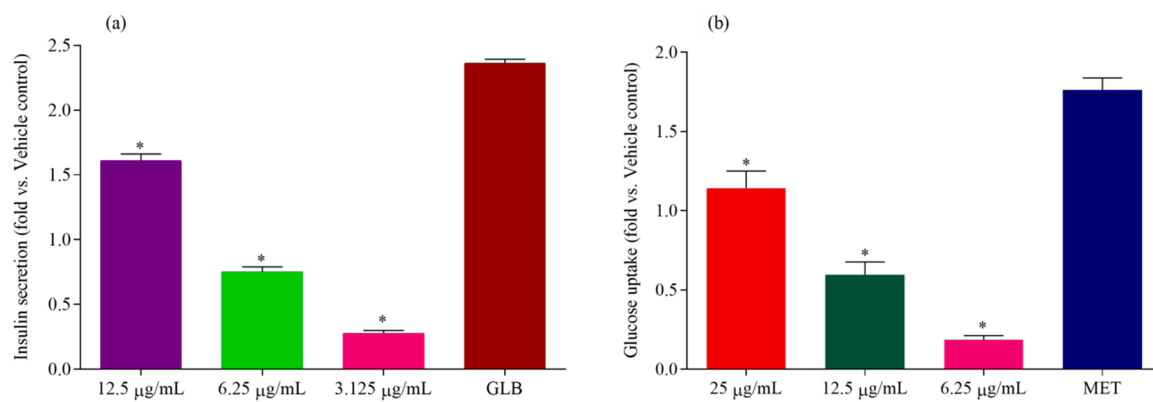


Fig. 4. (a) Insulin secretion and (b) Glucose uptake activities of the EN of *C. travancoricum* at different concentrations on MIN6 & L6 cell lines. Values are mean \pm S.D (n = 3) GLB - glibenclamide (12.5 µg/mL); MET – metformin (25 µg/mL). *P < 0.01 vs STD (GLB & MET).

Therefore, on the basis of the results, approximately one-fifth of the dose, i.e., 100 mg/kg b.wt., which was a considerably low concentration, was chosen for dose optimization study.

3.8. Dose optimization

Five different doses of EN of CT (6.25, 12.5, 25, 50 & 100 mg/kg b.wt.) were used for dose optimization on Wistar rats. The intraperitoneal injection of D-glucose elevated the blood glucose level in VC and other

groups at 30 min. Of these five doses, blood glucose level was effectively reduced at 12.5 mg/kg b.wt. compared to the other doses (30, 60 and 120 min) and VC (Fig. 5). Therefore, the dose of 12.5 mg/kg/b.wt. was selected for STZ-induced diabetic study as an effective dose and from which a 2-fold increased dose (25 mg/kg/b.wt.) and a 2-fold decreased dose (6.25 mg/kg/b.wt.) were used as high and low doses for further antidiabetic study.

Since EN of CT showed better *in vitro* antidiabetic activity, further *in vivo* antidiabetic study was conducted to establish the fact. The dose was

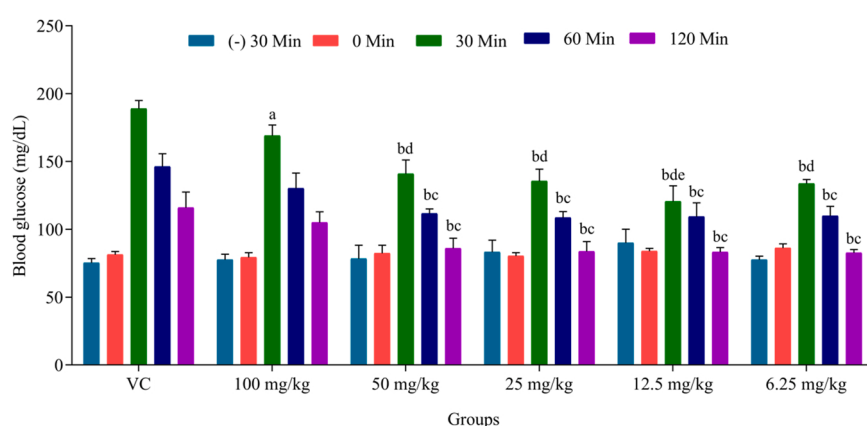


Fig. 5. Dose optimization of EN of *C. travancoricum*. VC-vehicle control; EN at different concentrations (100, 50, 25, 12.5 and 6.25 mg/kg b.wt.). Values are mean \pm S.D (n = 3). ^aP < 0.05 vs VC at respective time; ^bP < 0.01 vs VC at respective time; ^cP < 0.05 vs 100 mg/kg at respective time; ^dP < 0.01 vs 100 mg/kg at respective time; ^eP < 0.05 vs 50 mg/kg.

optimized and chosen for the Streptozotocin (STZ) induced diabetic study based on acute oral toxicity and dose optimization studies. Most of the studies have used either Alloxan or STZ to induce diabetes. Of these, the STZ-induced animal model is the most common and reliable method [75]. STZ induces diabetes mellitus in rodents through impairment of glucose oxidation and reduction of insulin biosynthesis and secretion [75–77]. The action of STZ-induced diabetes in rodents causes alkylation of DNA which produces reactive oxygen species and increased production of nitric oxide in the β -cells [75]. In the present study, elevated blood glucose level was observed in STZ induced Wistar rats due to the damage of pancreatic islets and death of β -cells caused by STZ.

3.9. Effect of EN on body weight and feed intake

The body weight changes in STZ-induced diabetic rats were measured on 0th, 14th and 28th days. The body weight was significantly ($P < 0.01$) reduced in diabetic animals than NC animals (Fig. 6). The decreased body weight in VC group indicates that surfactants did not have any effect. Due to impaired glycemic control, the body weight in diabetic animals was reduced. However, the body weight of EN (low, medium and high doses) and STD treated animals significantly ($p < 0.01$) increased on 28th day compared to DC and VC groups. Moreover, DC and VC groups did not gain body weight despite having increased feed intake compared to NC group (Table 3). The results revealed that EN treated animals reversed the excessive feed intake (polyphagia) to normal in a dose-dependent manner by controlling hyperglycemia.

Reduction of body weight observed in STZ-induced diabetic rats is due to impaired insulin action in the transformation of glucose into glycogen, inhibition of lipolysis and catabolism of fats [78,79]. In the present study, EN of CT and glibenclamide regained the reduced body weight of diabetic-induced rats by decreasing hyperglycemia, thus resulting in decreased feed intake.

3.10. Effect of EN on blood glucose level

Intraperitoneal injection of STZ triggered an increase in blood glucose level in the test animals (Fig. 7). The DC and VC groups showed a significant ($P < 0.01$) elevation in glucose level than NC. The EN (low, medium and high) and STD treated animals significantly ($p < 0.01$) decreased blood glucose level on 28th day than the DC group.

Elevated blood glucose level is the most common condition in diabetes. Reduced use of glucose by the tissues, higher level of hepatic

Table 3
Feed intake in different groups of animals.

Groups	Feed intake (g/day)		
	0 th day	14 th day	28 th day
NC	65.40 ± 1.03	68.11 ± 0.39	70.53 ± 3.03 *
DC	69.56 ± 8.83	80.50 ± 0.38	88.41 ± 8.29
VC	65.24 ± 1.62	80.42 ± 4.24	87.31 ± 4.27
STD	68.59 ± 2.32	70.65 ± 7.05	72.15 ± 4.29
Low	66.78 ± 2.33	80.39 ± 8.80	86.49 ± 4.03
Medium	67.92 ± 10.17	80.26 ± 7.76	83.75 ± 2.69
High	67.64 ± 6.89	73.37 ± 1.16	72.32 ± 4.06

NC - normal control; DC - disease control; VC - vehicle control; STD - glibenclamide at 5 mg/kg b.wt.; Low - EN at 6.25 mg/kg b.wt.; Medium - EN at 12.5 mg/kg b.wt.; High - EN at 25 mg/kg b.wt. Values are mean ± S.D (n = 6).

* $P < 0.01$ vs DC.

glycogenolysis, excessive gluconeogenesis and reduction in insulin secretion due to pancreatic β -cell damage are the major causes of hyperglycemia [80]. In the present study, the animals treated with EN of CT showed a significant ($p < 0.05$ & $p < 0.01$) reduction in blood glucose level in a dose-dependent manner. The blood glucose lowering effect might be due to the improved glucose uptake by the cells, enhanced insulin secretion and moderate inhibition of α -amylase and α -glucosidase enzymes which were supported by the *in vitro* studies. The responsible components of the EO which caused blood glucose lowering effects were predicted using *in silico* studies.

3.11. Effect of EN on blood glucose tolerance test

Results of intraperitoneal glucose tolerance test (IPGTT) and bar graph of area under the curve for IPGTT are displayed in Fig. 8a and 8b respectively. Maximum blood glucose level was reached at 30 min after intraperitoneal injection of glucose in DC and VC groups and persisted for up to 120 min ($p < 0.01$) as compared to NC. On the other hand, after oral administration of EN of CT, the maximum level of blood glucose reached within 30 min, but it almost reached the base level by 120 min ($p < 0.01$) compared to DC and VC groups.

3.12. Effect of EN on plasma insulin

After 28 days of treatment of EN of CT, the plasma insulin level was measured. A significant decrease in insulin level was observed in the DC group ($P < 0.01$) compared to the NC group. Similarly, reduced insulin

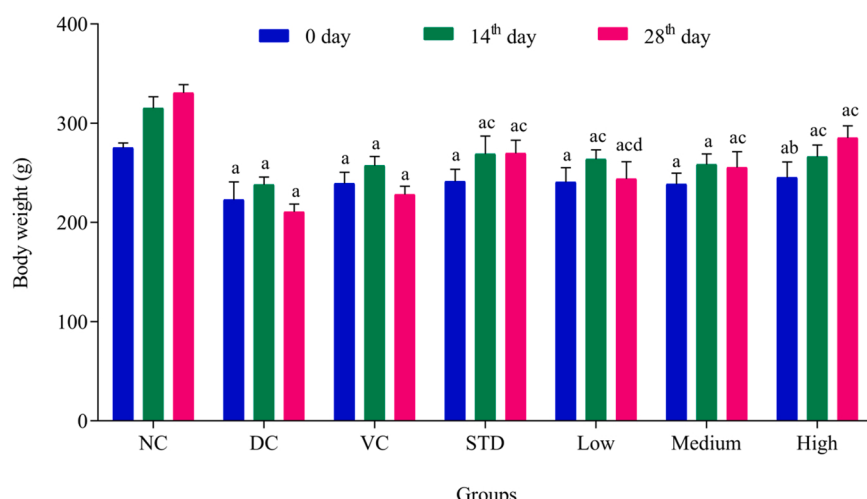


Fig. 6. Effect of EN of *C. travancoricum* on body weight. NC - normal control; DC - disease control; VC - vehicle control; STD - glibenclamide at 5 mg/kg b.wt.; Low at 6.25 mg/kg b.wt.; Medium - EN at 12.5 mg/kg b.wt.; High - EN at 25 mg/kg b.wt. Values are mean ± S.D (n = 6). ^a $P < 0.01$ vs NC; ^b $P < 0.05$ vs DC; ^c $P < 0.01$ vs DC; ^d $P < 0.01$ vs STD.

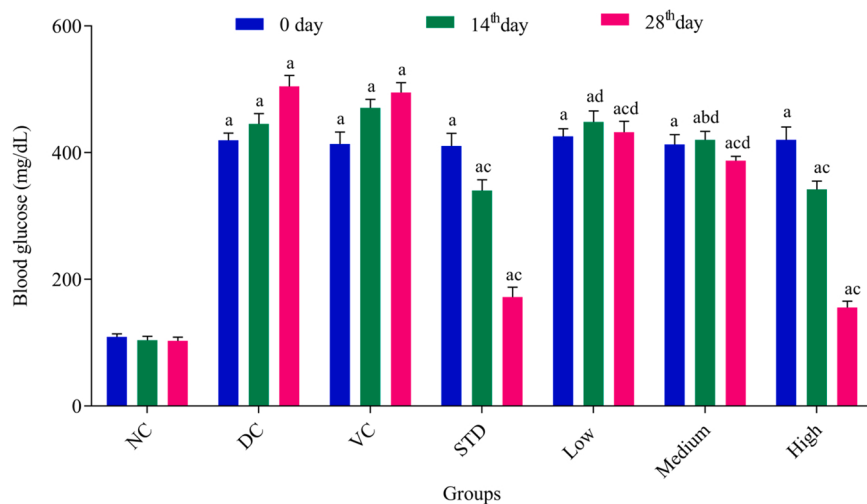


Fig. 7. Effect of EN of *C. travancoricum* on blood glucose level. NC - normal control; DC - disease control; VC - vehicle control; STD – glibenclamide at 5 mg/kg b.wt.; Low - EN at 6.25 mg/kg b.wt.; Medium - EN at 12.5 mg/kg b.wt.; High - EN at 25 mg/kg b.wt. Values are mean \pm S.D (n = 6); ^aP < 0.01 vs NC; ^bP < 0.05 vs DC; ^cP < 0.01 vs DC; ^dP < 0.01 vs STD.

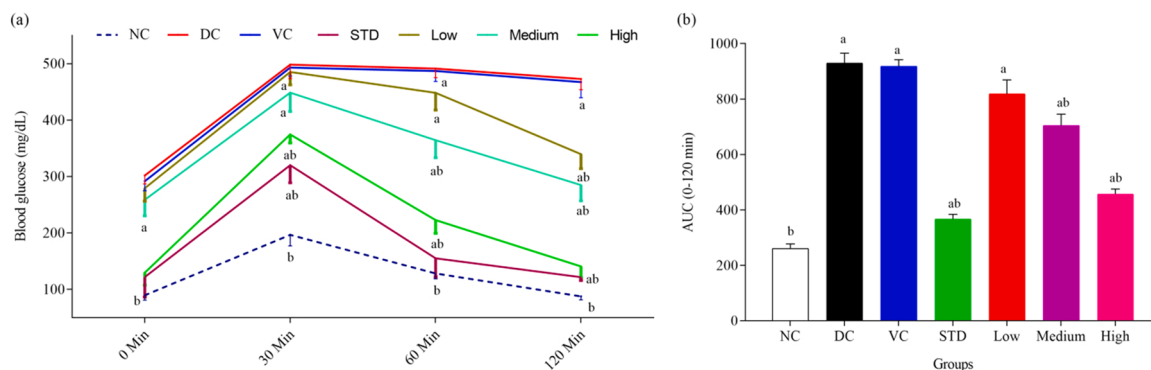


Fig. 8. Effect of EN of *C. travancoricum* on (a) intraperitoneal glucose tolerance test (IPGTT) and (b) area under the curve for IPGTT. NC - normal control; DC - disease control; VC - vehicle control; STD – glibenclamide at 5 mg/kg b.wt.; Low - EN at 6.25 mg/kg b.wt.; Medium - EN at 12.5 mg/kg b.wt.; High - EN at 25 mg/kg b.wt. Values are mean \pm S.D (n = 6); ^aP < 0.05 vs NC; ^bP < 0.05 vs DC.

levels observed in the VC group showed that the vehicle had no effect. However, STZ induced animals treated with EN of CT (low, medium and high doses) and STD showed significant ($p < 0.01$) elevation in insulin

level compared to the DC group (Fig. 9).

3.13. Effect of EN on serum liver enzymes

Serum ALP, AST and ALT levels in the DC and VC groups were significantly ($p < 0.05$) higher than the NC group. However, on treatment with EN for 28 days, the high dose group exhibited significant ($p < 0.05$) reduction in serum ALP level compared to the DC group. Similarly, AST and ALT levels were also reduced in the medium and high dose groups (Fig. 10).

In diabetic condition, hyperglycemia is associated with dyslipidemia which causes atherosclerosis and cardiovascular disease. STZ-induced diabetes increases glucose level which causes remarkable variations in lipids level. The deficiency of insulin linked with diabetes triggers the hormone-sensitive lipase which releases free fatty acid deposited in the adipose tissue ruling to elevate the serum lipids [81]. The increased levels of TC, TG, LDL and decreased level of HDL are common in diabetic conditions [82]. The same trend was observed in the present investigation. This curative effect might be due to EN of CT improving insulin secretion which controls the release of free fatty acid in the adipose tissue.

STZ-induced diabetes causes hepatic damage by the rupture of hepatocytes, which bring out transaminases causing decreased liver function [83]. Liver function enzymes namely, AST, ALT, and ALP are

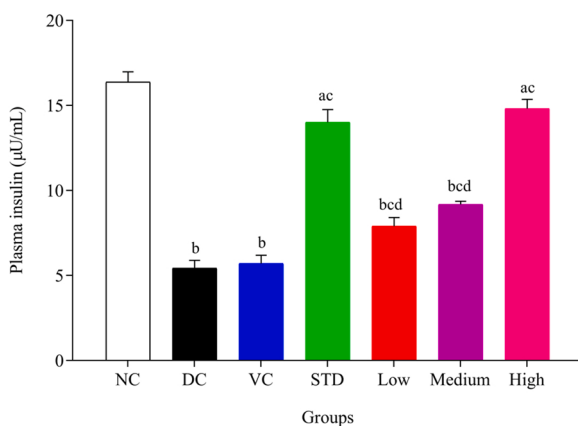


Fig. 9. Effect of EN of *C. travancoricum* on plasma insulin level. NC - normal control; DC - disease control; VC - vehicle control; STD – glibenclamide at 5 mg/kg b.wt.; Low - EN at 6.25 mg/kg b.wt.; Medium - EN at 12.5 mg/kg b.wt.; High - EN at 25 mg/kg b.wt. Values are mean \pm S.D (n = 6). ^aP < 0.05 vs NC; ^bP < 0.01 vs DC; ^cP < 0.01 vs DC; ^dP < 0.01 vs STD.

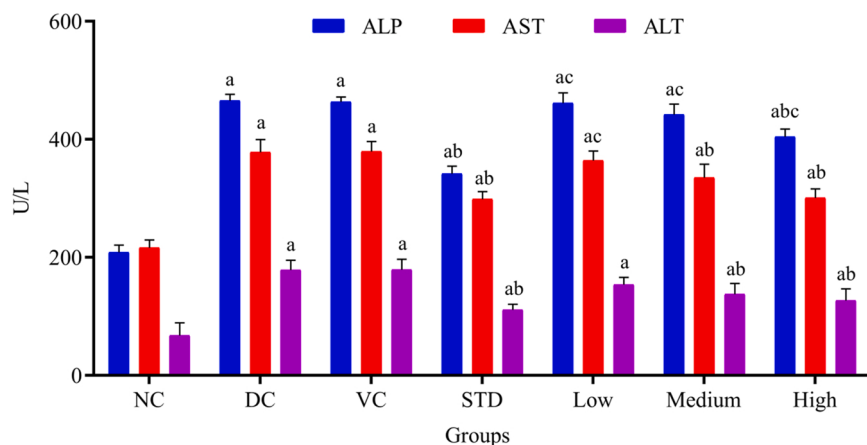


Fig. 10. Effect of EN of *C. travancoricum* on serum liver enzymes on 28th day. ALP – alkaline phosphatase; AST – aspartate amino transferase; ALT – alanine amino transferase. NC - normal control; DC - disease control; VC - vehicle control; STD - glibenclamide at 5 mg/kg b.wt.; Low - EN at 6.25 mg/kg b.wt.; Medium - EN at 12.5 mg/kg b.wt.; High - EN at 25 mg/kg b.wt. Values are mean \pm S.D (n = 6). ^aP < 0.01 vs NC; ^bP < 0.01 vs DC; ^cP < 0.01 vs STD.

released in high amounts into the bloodstream from the liver cytoplasm as a consequence of hepatocytes membrane permeability [84]. The administration of EN of CT reduced the amount of serum AST, ALT, and ALP levels, which might be due to the antioxidant activity of the EO of CT.

3.14. Effect of EN on serum lipids

Administration of EN of CT for 28 days, significant ($p < 0.05$) reduction in the TC level was observed in high dose group compared to the DC group. Triglycerides level was increased in DC and VC groups compared to the NC group. There was a significant decrease ($p < 0.05$) in triglycerides level in medium and high dose groups compared to the DC group. As the study was performed for 28 days, no significant difference in the level of HDL and LDL was observed (Fig. 11).

3.15. Effect of EN on pancreatic islets

No pathological alteration in the pancreatic cellular architecture was exhibited in the NC. The DC group exhibited dispersed necrotic changes in the pancreas as an outcome of the remarkable decrease in the number of β -cells in the Langerhans islets. A similar effect was observed in the VC group thus suggesting no role of surfactants on the pancreas. The

glibenclamide (STD) treated group exhibited a moderate enhancement of islets of Langerhans and also β -cells. The EN of CT exposed a development in islets of Langerhans and a definite improvement in the β -cells in dose dependent manner. Moreover, EN of CT at high dose showed regeneration of β -cells as compared to the DC group (Fig. 12).

In the present study, a significant reduction ($P < 0.01$) in the plasma insulin level was observed in the DC group compared to the NC group. However, after treatment with EN of CT, the insulin level was increased in the DC group. This effect might be due to the increased insulin secretion from β cells, which is supported through *in vitro* insulin secretion assay. The improved insulin secretion might be due to the regeneration of β cells or increased insulin secretion from remaining β cells thereby improving insulin sensitivity [85]. In the present investigation, a minimum area of the β cells was observed in the DC group with the least number of β cells. But in EN of CT treated groups, development of β cell mass was observed. The probable reason might be the EN of CT which stimulated the regeneration of β cells.

3.16. Ligand and protein structures used in docking studies

The ligands used for molecular docking studies are given in fig. S1. The 3D structures of α -amylase (1HNY), α -glucosidase (2ZEO), insulin receptor (1IR3) and protein involved in insulin secretion – glucagon-like

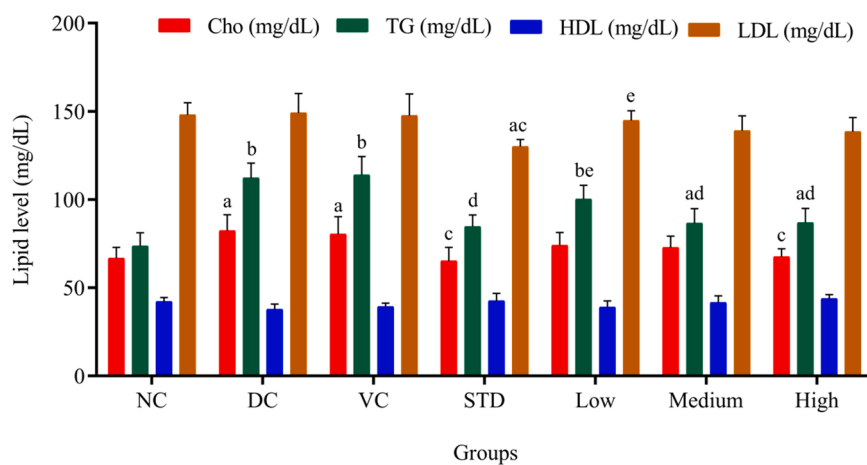


Fig. 11. Effect of EN of *C. travancoricum* on serum lipid levels on 28th day. Cho - total cholesterol; TG - triglycerides; HDL - high-density lipoproteins; LDL - low-density lipoproteins. NC - normal control; DC - disease control; VC - vehicle control; STD - glibenclamide at 5 mg/kg b.wt.; Low - EN at 6.25 mg/kg b.wt.; Medium - EN at 12.5 mg/kg b.wt.; High - EN at 25 mg/kg b.wt. Values are mean \pm S.D (n = 6). ^aP < 0.05 vs NC; ^bP < 0.01 vs NC; ^cP < 0.05 vs STD; ^dP < 0.01 vs DC;

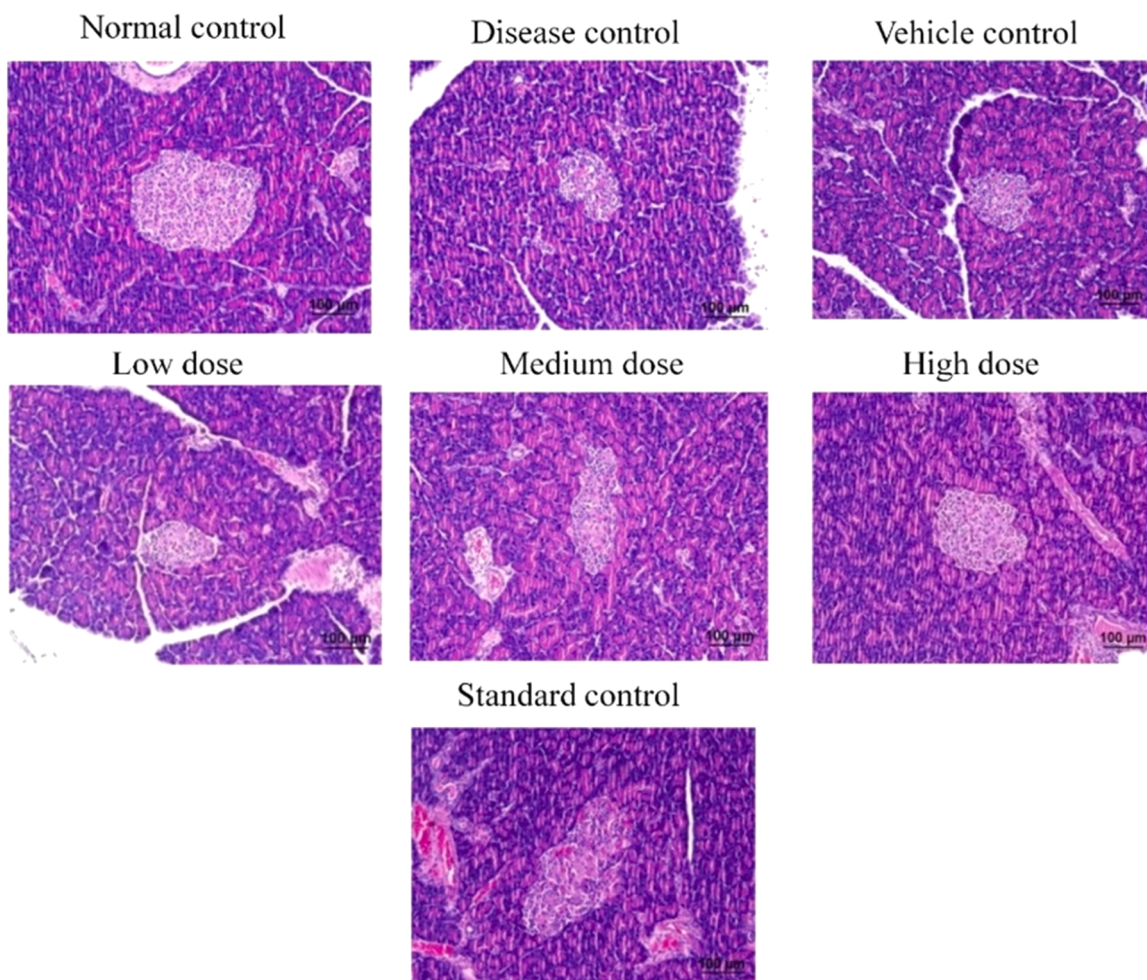


Fig. 12. Effect of EN of *C. travancoricum* on pancreatic islets. Low dose - EN at 6.25 mg/kg b.wt.; Medium dose - EN at 12.5 mg/kg b.wt.; High dose - EN at 25 mg/kg b.wt.; Standard control – glibenclamide at 5 mg/kg b.wt.

peptide – 1 (2ZGM) (Fig. S2) were retrieved from the protein data bank (PDB) (<http://www.rcsb.org>) and these were chosen as the molecular target for this docking studies. The corresponding gene symbols are AMY2A, GSJ, INSR and GLP1R respectively. The active site residues of these proteins were predicted using Schrödinger sitemap and given in table S1.

3.17. Molecular docking and MM-GB/SA

Glide XP docking was performed for the 42 ligands and the docking scores are tabulated in tables S2–S5. Each ligand was docked in different poses, and the pose with the lowest score was selected for further analysis. It was found that each docked ligand forms strong interaction (including hydrogen bond) with the active site amino acid residues in the cleft.

The docked pose of Glide output was given as the input for MM-GB/SA to predict the accurate binding free energy. Prime MM-GB/SA uses the VSGB 2.0 solvation model. The energy was calculated by the Prime algorithm. Calculated MM-GBSA values are tabulated in table S2–S5. The lead compounds with highest negative binding energy and their binding interactions with target proteins were assumed (Table 4) to be the reason for the synergic activity of the whole EO in the respective *in vitro* and *in vivo* analysis. Briefly, α -amylase inhibitory activity of CT was imparted due to the inhibitory effect of δ -cadinene (Table S2 & Fig. 13A). In case of α -glucosidase inhibition, elemol showed inhibitory interactions (Table S3 & Fig. 13D). Spathulenol showed agonist interaction with insulin receptor imparting its activity on cells (Table S4 &

Table 4

Table shows the compounds affinity with interacting active site residues of proteins.

S. No.	Proteins (PDB ID)	Ligands	Interacting active site residues
1	α -Amylase (1HNY)	δ -Cadinene	No hydrogen bonding interaction, strong hydrophobic interaction
2	α -Glucosidase (2ZE0)	Elemol	ASN61, ASP326
3	Insulin receptor (1IR3)	Spathulenol	ARG1039, LYS1168
4	Glut-4	Spathulenol	ASN427, ASN431
5	4ZGM	α -Copaen-11-ol	No hydrogen bonding interaction, Strong hydrophobic interaction

Fig. 13B). α -Copaen-11-ol act as GLP-1 agonist to induce the secretion of insulin (Table S5 & Fig. 13C). Among the 42 chemical compounds from EO of CT, the above mentioned four compounds have high affinity with the four different receptors against diabetes mellitus. Based on the docking results, it can be concluded that *in vitro* and *in vivo* antidiabetic effect of CT may be due to these lead compounds.

After confirmation of *in vitro* and *in vivo* antidiabetic effect of the EN of CT, molecular docking study was performed to find the active compounds which are responsible for antidiabetic activity. Fig. 14 shows the possible lead components which interact with the proteins involved in the glucose homeostasis. Based on the outcome, these components alone

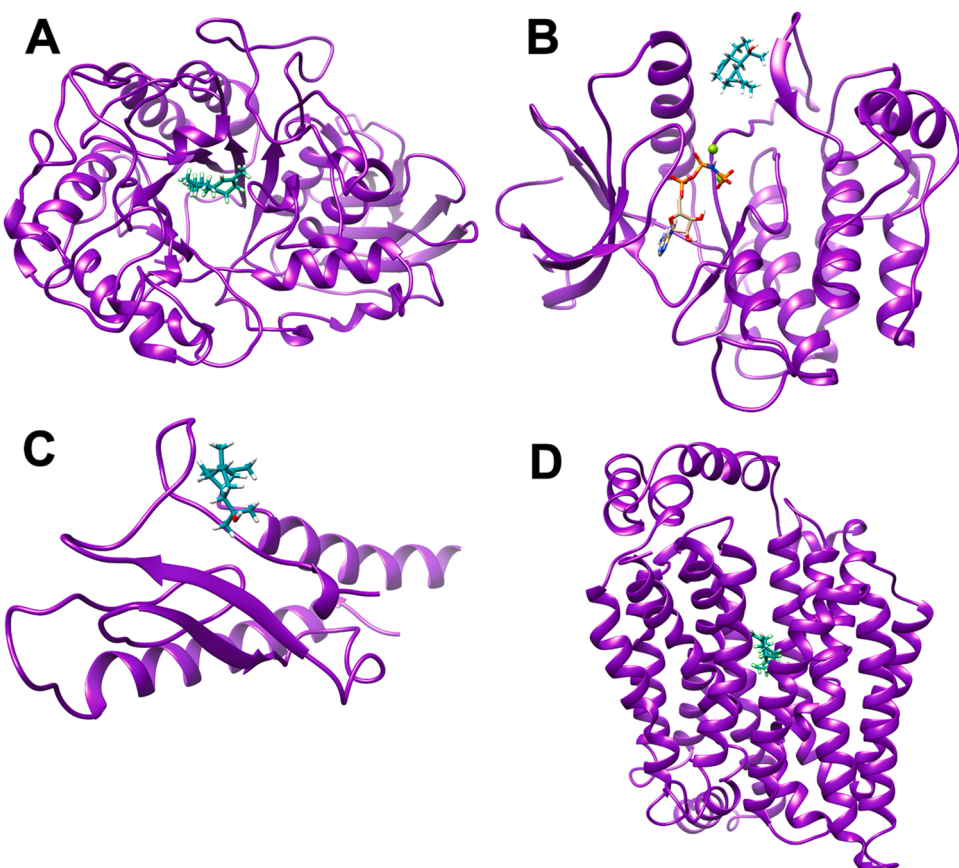


Fig. 13. Interaction and binding poses of respective compounds with proteins A) δ -cadinene - α -amylase; B) spathulenol - insulin receptor; C) α -cpaen-11-ol - GLP-1; D) elemol - α -glucosidase. Their respective PDB IDs are 1HNY A) 1IR3 B) 4ZGM C) 2ZE0 D). The purple colored ribbon structures indicate the three dimensional structure of proteins and the green sticks indicate the ligand.

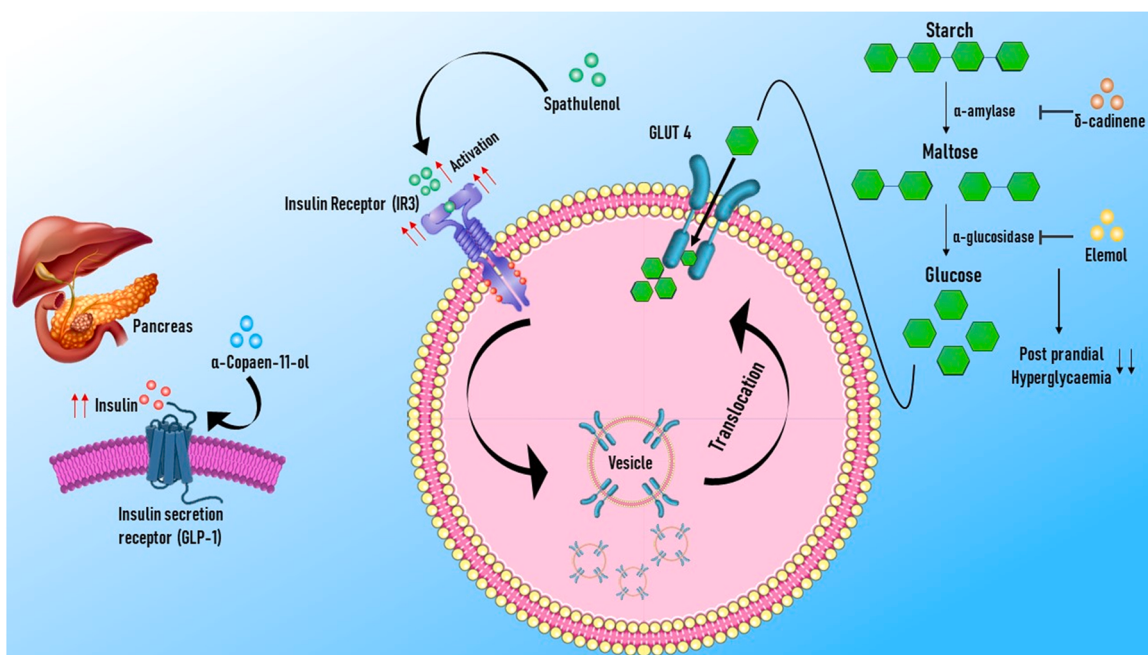


Fig. 14. Schematic diagram of the possible antidiabetic components from *C. travancoricum* and its interaction with different proteins involved in glucose homeostasis.

can be evaluated for their antidiabetic effect through *in vitro* and *in vivo* approach. Apart from these components, some other components from CT such as safrole and linalool have already been proved to possess better antidiabetic effect *in vivo* animal model [86,87]. However, in molecular docking study, δ -cadinene, elemol, Spathulenol α -Copaen-11-ol showed better interaction than safrole and linalool. Overall, the antidiabetic effect of the EN of CT might be due to the synergistic activity of either the proposed components or mixture of multiple components via different modes of mechanism.

4. Conclusion

To the best of our knowledge, this is the first report on antidiabetic activity of the wild cinnamon, CT. As an effort to solve the dissolvability and bioavailability of EO in water based medium, a suitable method of EN preparation was formulated and characterized. The *in vitro* assays namely, α -amylase and α -glucosidase inhibitory assays, glucose uptake using L6 cell line and insulin secretion assay using MIN6 cell line proved the antidiabetic potential of CT. Though α -amylase and α -glucosidase inhibitory assays exhibited moderate activity of EN, it showed excellent glucose uptake and insulin secretion activities. The moderate α -amylase and α -glucosidase inhibitory activity is often preferred in diabetic condition in spite of complete inhibition of these enzymes. The *in vivo* results were correlated with the *in vitro* and *in silico* results. Molecular docking studies resolved the probable EO components responsible for the antidiabetic action. Overall, EN of CT showed a therapeutic effect against diabetes mellitus.

Data availability

Data related to chemical analysis and molecular docking is provided in supplementary file. Further data will be made available on request.

Acknowledgments

RM is grateful to the Science and Engineering Research Board, Department of Science & Technology, Government of India, New Delhi (Grant No. SB/FT/LS-300/2012) for financial support and to the Management and Principal of Ayya Nadar Janaki Ammal College, Sivakasi, India for support and encouragement. The authors also thank Dr. Srivivasan Vedantham (Associate Director, MedGenome) for the cell culture facilities. VS thanks the Vice-Chancellor, SASTRA Deemed University, India for providing facilities and Teaching Assistant Fellowship. VS is also grateful to Mr. R. Narasimhan and Mr. T.V. Ramadhegian for financial support to complete the *in vivo* study.

Declaration of interest

None.

Appendix A. Supporting information

Supplementary data associated with this article can be found in the online version at [doi:10.1016/j.procbio.2022.04.031](https://doi.org/10.1016/j.procbio.2022.04.031).

References

- [1] T.R. Tomlinson, O. Akerele, Medicinal Plants: Their Role in Health and Biodiversity, University of Pennsylvania Press, Philadelphia, 1998.
- [2] P.O. Osadebe, E.O. Uchenna, P. Uzor, Natural products as potential sources of antidiabetic drugs, Br. J. Pharm. Res. 4 (2014) 2075–2095, <https://doi.org/10.9734/BJPR/2014/8382>.
- [3] M. Neelesh, J. Sanjay, M. Sapna, Antidiabetic potential of medicinal plants, Acta Poloniae Pharm. Drug Res. 67 (2010) 113–118.
- [4] S. Dewanjee, A.K. Das, R. Sahu, M. Gangopadhyay, Anti-diabetic activity of *Diospyros peregrina* fruit: effect on hyperglycemia, hyperlipidemia and augmented oxidative stress in experimental type 2 diabetes, Food Chem. Toxicol. 47 (2009) 2679–2685, <https://doi.org/10.1016/j.fct.2009.07.038>.
- [5] P. Shokeen, P. Anand, Y.K. Murali, V. Tandon, Antidiabetic activity of 50% ethanolic extract of *Ricinus communis* and its purified fractions, Food Chem. Toxicol. 46 (2008) 3458–3466, <https://doi.org/10.1016/j.fct.2008.08.020>.
- [6] C.J. Bailey, C. Day, Traditional plant medicines as treatments for diabetes, Diabetes Care 12 (1989) 553–564, <https://doi.org/10.2337/diacare.12.8.553>.
- [7] K.G. Alberti, P.Z. Zimmet, Definition, diagnosis and classification of diabetes mellitus and its complications. Part 1: diagnosis and classification of diabetes mellitus provisional report of a WHO consultation, Diabetes Med. 15 (1998) 539–553, [https://doi.org/10.1002/\(SICI\)1096-9136\(199807\)15:7<539::AID-DIA668>3.0.CO;2-S](https://doi.org/10.1002/(SICI)1096-9136(199807)15:7<539::AID-DIA668>3.0.CO;2-S).
- [8] N.H. Cho, J.E. Shaw, S. Karuranga, Y. Huang, J.D. da Rocha Fernandes, A. W. Ohlrogge, B. Malanda, IDF diabetes atlas: global estimates of diabetes prevalence for 2017 and projections for 2045, Diabetes Res. Clin. Pract. 138 (2018) 271–281, <https://doi.org/10.1016/j.diabres.2018.02.023>.
- [9] J.C.N. Chan, V. Malik, W. Jia, T. Kadokawa, C.S. Yajnik, K.H. Yoon, F.B. Hu, Diabetes in Asia: epidemiology, risk factors, and pathophysiology, JAMA 301 (2009) 2129–2140, <https://doi.org/10.1001/jama.2009.726>.
- [10] M.J. Meneses, B.M. Silva, M. Sousa, R. Sa, P.F. Oliveira, M.G. Alves, Antidiabetic drugs: mechanisms of action and potential outcomes on cellular metabolism, Curr. Pharm. Des. 21 (2015) 3606–3620, <https://doi.org/10.2174/138161282166150710145753>.
- [11] S.E. Inzucchi, R.M. Bergenstal, J.B. Buse, M. Diamant, E. Ferrannini, M. Nauck, A. L. Peters, A. Tsapas, R. Wender, D.R. Matthews, Management of hyperglycemia in type 2 diabetes: a patient-centered approach: position statement of the American diabetes association (ADA) and the European association for the study of diabetes (EASD), Diabetes Care 35 (2012) 1364–1379, <https://doi.org/10.2337/dc12-0413>.
- [12] T. Buchholz, M.F. Melzig, Medicinal plants traditionally used for treatment of obesity and diabetes mellitus – screening for pancreatic lipase and α -amylase inhibition, Phytother. Res. 30 (2016) 260–266, <https://doi.org/10.1002/ptr.5525>.
- [13] B. Salehi, A. Ata, N.V. Anil Kumar, F. Sharopov, K. Ramírez-Alarcón, A. Ruiz-Ortega, S.A. Ayatollahi, P.V.T. Fokou, F. Kobarfard, Z.A. Zakaria, M. Iriti, Y. Taheri, M. Martorell, A. Sureda, W.N. Setzer, A. Durazzo, M. Lucarini, A. Santini, R. Capasso, E.A. Ostrander, M.I. Atta-ur-Rahman, W.C. Choudhary, J. Cho, Sharifi-Rad, Antidiabetic potential of medicinal plants and their active components, Biomolecules 9 (2019) 1–121, <https://doi.org/10.3390/biom9100551>.
- [14] W. Kooti, M. Moradi, S. Akbari, N. Sharafi-Ahvaz1, M. Asadi-Samani, D. Ashtary-Larky, Therapeutic and pharmacological potential of *Foeniculum vulgare* Mill: a review, J. Herbmed. Pharm. 4 (2015) 1–9.
- [15] M. Bnouham, A. Ziyyat, H. Mekhfi, A. Tahri, Medicinal plants with potential antidiabetic activity – a review of ten years of herbal medicine research (1990–2000), Int. J. Diabetes Metab. 14 (2006) 1–25, <https://doi.org/10.1159/000497588>.
- [16] R.J. Marles, N.R. Farnsworth, Antidiabetic plants and their active constituents, Phytomed 2 (1995) 137–189, [https://doi.org/10.1016/S0944-7113\(11\)80059-0](https://doi.org/10.1016/S0944-7113(11)80059-0).
- [17] A. Mollica, A. Stefanucci, G. Zengin, M. Locatelli, G. Macedonio, G. Orlando, C. Ferrante, L. Menghini, L. Recinella, S. Leone, A. Chiavaroli, L. Leporini, C. Di Nisio, L. Brunetti, E. Tayrab, I. Ali, T.H. Musa, H.H. Musa, A.A. Ahmed, Polyphenolic composition, enzyme inhibitory effects ex-vivo and in-vivo studies on two Brassicaceae of north-central Italy, Biomed. Pharm. 107 (2018) 129–138, <https://doi.org/10.1016/j.bioph.2018.07.169>.
- [18] A. Mollica, G. Zengin, M. Locatelli, A. Stefanucci, G. Macedonio, G. Bellagamba, O. Onaolapo, A. Onaolapo, F. Azeez, A. Ayileka, E. Novellino, An assessment of the nutraceutical potential of *Juglans regia* L. leaf powder in diabetic rats, Food Chem. Toxicol. 107 (2017) 554–564, <https://doi.org/10.1016/j.fct.2017.03.056>.
- [19] A. Mollica, G. Zengin, M. Locatelli, A. Stefanucci, A. Mocan, G. Macedonio, S. Carradori, O. Onaolapo, A. Onaolapo, J. Adegoke, M. Olaniyan, A. Aktumsek, E. Novellino, Anti-diabetic and anti-hyperlipidemic properties of *Capparis spinosa* L.: *In vivo* and *in vitro* evaluation of its nutraceutical potential, J. Funct. Foods 35 (2017) 32–42, <https://doi.org/10.1016/j.jff.2017.05.001>.
- [20] A.A. Ahmed, A. Mollica, A. Stefanucci, E. Tayrab, H. Ahmed, M.E.A. Essa, Gum Arabic improves the reproductive capacity through upregulation of testicular glucose transporters (GLUTs) mRNA expression in Alloxan induced diabetic rat, Bioact. Carbohydr. Diet. Fibre 22 (2020) 2212–6198, <https://doi.org/10.1016/j.bcf.2020.100218>.
- [21] A.J.G.H. Kostermans, *Cinnamomum*, in: F.R. Fosberg (Ed.), A Revised Handbook to the Flora of Ceylon vol.9, Amerind Publishing Co., New Delhi, 1995, pp. 112–129.
- [22] T.S. Nayar, A.R. Beegam, M. Sibi, Flowering Plants of the Western Ghats, India, Jawaharlal Nehru Tropical Botanic Garden and Research Institute, Thiruvananthapuram, India, 2014.
- [23] E.J. Verspohl, K. Bauer, E. Neddermann, Antidiabetic effect of *Cinnamomum cassia* and *Cinnamomum zeylanicum* *In vivo* and *In vitro*, Phytother. Res. 19 (2005) 203–206, <https://doi.org/10.1002/ptr.1643>.
- [24] P.S. Babu, S. Prabuseenivasan, S. Ignacimuthu, Cinnamaldehyde – a potential antidiabetic agent, Phytomed 14 (2007) 15–22, <https://doi.org/10.1016/j.phymed.2006.11.005>.
- [25] R.A. Anderson, C.L. Broadhurst, M.M. Polansky, W.F. Schmidt, A. Khan, V. P. Flanagan, N.W. Schoene, D.J. Graves, Isolation and characterization of polyphenol Type-A polymers from cinnamon with insulin-like biological activities, J. Agric. Food Chem. 52 (2004) 65–70, <https://doi.org/10.1021/jf034916b>.
- [26] K.J. Jarvill-Taylor, R.A. Anderson, D.J. Graves, A hydroxychalcone derived from cinnamon functions as a mimetic for insulin in 3T3-L1 adipocytes, J. Am. Coll. Nutr. 20 (2001) 327–336, <https://doi.org/10.1080/07315724.2001.10719053>.
- [27] W. Kim, L.Y. Khil, R. Clark, S.H. Bok, E.E. Kim, S. Lee, H.S. Jun, W.J. Yoon, Naphthalenemethyl ester derivative of dihydroxyhydrocinnamic acid, a component of cinnamon, increases glucose disposal by enhancing translocation of

- glucose transporter 4, *Diabetologia* 49 (2006) 2437–2448, <https://doi.org/10.1007/s00125-006-0373-6>.
- [28] S. Adisakwattana, O. Lerdsuwankij, U. Poputtachai, A. Minipun, C. Suparpprom, Inhibitory activity of cinnamom bark species and their combination effect with acarbose against intestinal α -glucosidase and pancreatic α -amylase, *Plant Foods Hum. Nutr.* 66 (2011) 143–148, <https://doi.org/10.1007/s11130-011-0226-4>.
- [29] G.M. Lin, Y.H. Chen, P.L. Yen, S.T. Chang, Antihyperglycemic and antioxidant activities of twig extract from *Cinnamomum osmophloeum*, *J. Tradit. Complement. Med.* 6 (2016) 281–288, <https://doi.org/10.1016/j.jtcme.2015.08.005>.
- [30] V. Sriramavaratharajan, R. Murugan, Cumin scented leaf essential oil of *Cinnamomum chemungianum*: compositions and their in vitro antioxidant, α -amylase, α -glucosidase and lipase inhibitory activities, *Nat. Prod. Res.* 32 (2018) 2081–2084, <https://doi.org/10.1080/14786419.2017.1360884>.
- [31] V. Sriramavaratharajan, R. Murugan, Chemical profile of leaf essential oil of *Cinnamomum walaiwarense* and comparison of its antioxidant and hypoglycemic activities with the major constituent benzyl benzoate, *Nat. Prod. Commun.* 13 (2018) 779–782, <https://doi.org/10.1177/1934578x1801300633>.
- [32] V. Sriramavaratharajan, R. Murugan, Screening of chemical composition, in vitro antioxidant, α -amylase and α -glucosidase inhibitory activities of the leaf essential oils of *Cinnamomum wightii* from different populations, *Nat. Prod. Commun.* 13 (2018) 1539–1542, <https://doi.org/10.1177/1934578x1801301132>.
- [33] V. Sriramavaratharajan, R. Murugan, Evaluation of chemical composition, antioxidant and anti-hyperglycemic activities of the essential oil based nanoemulsions of *Cinnamomum litseifolium*, *Nat. Prod. Res.* 33 (2019) 2430–2433, <https://doi.org/10.1080/14786419.2018.1446137>.
- [34] M. Maridass, B. Victor, Composition of essential oil and antimicrobial activity of *Cinnamomum travancoricum* from India, *Chem. Nat. Compd.* 45 (2009) 439–440, <https://doi.org/10.1007/s10600-009-9319-9>.
- [35] M. Maridass, Hepatoprotective activity of barks extract of six *Cinnamomum* species on carbon tetrachloride-induced in Albino rats, *Folia Med. Indones.* 45 (2009) 204–207.
- [36] M. Maridass, Evaluation of brine shrimp lethality of *Cinnamomum* species, *Ethnobot. Leafl.* 12 (2008) 772–775.
- [37] M. Maridass, Screening of antifungal activities of barks of *Cinnamomum* species, *Thai. J. Pharm. Sci.* 33 (2009) 137–143.
- [38] I.P. Tripathi, Chemistry, Biochemistry and Ayurveda of Indian Medicinal Plants. Indore, India, International E Publication, 2010.
- [39] V. Sriramavaratharajan, J. Stephan, V. Sudha, R. Murugan, Leaf essential oil of *Cinnamomum agasthyamalayanum* from the Western Ghats, India – a new source of camphor, *Ind. Crops Prod.* 86 (2016) 259–261, <https://doi.org/10.1016/j.indcrop.2016.03.054>.
- [40] R.P. Adams, Identification of Essential Oil Components by Gas Chromatography/ Quadrupole Mass Spectroscopy, fourth ed., Allured Publishing Corporation, Carol Stream, Illinois, USA, 2007.
- [41] M. Ilamathi, S. Santhosh, V. Sivaramakrishnan, Artesunate as an anti-cancer agent targets Stat-3 and favorably suppresses hepatocellular carcinoma, *Curr. Top. Med. Chem.* 16 (2016) 2453–2463, <https://doi.org/10.2174/1568026616666160212122820>.
- [42] Y. Sha, Y. Shi, B. Niu, Q. Chen, Cochinichinenin C, a potential nonpolypeptide anti-diabetic drug, targets a glucagon-like peptide-1 receptor, *RSC Adv.* 7 (2017) 49015–49023, <https://doi.org/10.1039/C7RA09470A>.
- [43] L. Kozma, K. Baltensperger, J. Klarlund, A. Porras, E. Santos, M.P. Czech, The ras signaling pathway mimics insulin action on glucose transporter translocation, *Proc. Natl. Acad. Sci. USA* 90 (1993) 4460–4464, <https://doi.org/10.1073/pnas.90.10.4460>.
- [44] OECD, Test guideline 425, Acute oral toxicity test: the up and down procedure. OECD Guidelines for the Testing of Chemicals, Organization for Economic Cooperation & Development, 2001.
- [45] M. El Kabbouai, A. Chda, Q. Azdad, N. Mejrhit, L. Aarab, R. Bencheikh, A. Tazi, Evaluation of hypoglycemic and hypolipidemic activities of aqueous extract of *Cistus ladaniferusin streptozotocin-induced diabetic rats*, *Asian Pac. J. Trop. Biomed.* 6 (2016) 1044–1049, <https://doi.org/10.1016/j.apbt.2016.09.005>.
- [46] S. Kumar, R. Kumari, S. Mishra, Pharmacological properties and their medicinal uses of *Cinnamomum*: a review, *J. Pharm. Pharm.* 71 (2019) 1735–1761, <https://doi.org/10.1111/jphp.13173>.
- [47] R. Ananthkrishnan, E.S. Santhoshkumar, K.B. Rameshkumar, Comparative chemical profiles of essential oil constituents of eight wild *Cinnamomum* species from the Western Ghats of India, *Nat. Prod. Commun.* 13 (2018) 621–625, <https://doi.org/10.1177/1934578x1801300525>.
- [48] A.M. Sandigawad, C.G. Patil, Isolation and characterization of alkaloids from *Cinnamomum Scha* (Lauraceae) species, *Adv. Biores.* 2 (2011) 90–91.
- [49] A. Acevedo-Fani, R. Soliva-Fortuny, O. Martín-Beloso, Nanoemulsions as edible coatings, *Curr. Opin. Food Sci.* 15 (2017) 43–49, <https://doi.org/10.1016/j.cofs.2017.06.002>.
- [50] A. Acevedo-Fani, L. Salvia-Trujillo, M.A. Rojas-Graü, O. Martín-Beloso, Edible films from essential-oil-loaded nanoemulsions: physicochemical characterization and antimicrobial properties, *Food Hydrocoll.* 47 (2015) 168–177, <https://doi.org/10.1016/j.foodhyd.2015.01.032>.
- [51] S.S. Lim, M.Y. Baik, E.A. Decker, L. Henson, L.M. Popplewell, D.J. McClements, S. J. Cho, Stabilization of orange oil-in-water emulsions: a new role for ester gums as an Ostwald ripening inhibitor, *Food Chem.* 128 (2011) 1023–1028, <https://doi.org/10.1016/j.foodchem.2011.04.008>.
- [52] M.I. Guerra-Rosas, J. Morales-Castro, L.A. Ochoa-Martinez, L. Salvia-Trujillo, O. Martín-Beloso, Long term stability of food-grade nanoemulsions from high methoxyl pectin containing essential oils, *Food Hydrocoll.* 52 (2016) 438–446, <https://doi.org/10.1016/j.foodhyd.2015.07.017>.
- [53] M. Gera, N. Sharma, M. Ghosh, D.L. Huynh, S.J. Lee, T. Min, T. Kwon, D.K. Jeong, Nanoformulations of curcumin: an emerging paradigm for improved remedial application, *Oncotarget* 8 (2017) 66680–66698, <https://doi.org/10.18632/oncotarget.19164>.
- [54] Z. Nouri, M. Hajialyani, Z. Izadi, R. Bahrami-Soltani, M.H. Farzaei, M. Abdollahi, Nanophytomedicines for the prevention of metabolic syndrome: a pharmacological and biopharmaceutical review, *Front. Bioeng. Biotech.* 8 (2020) 425, <https://doi.org/10.3389/fbioe.2020.00425>.
- [55] D.S. Bernardi, T.A. Pereira, N.R. Maciel, J. Bortoloto, G.S. Viera, G.C. Oliveira, P. A. Rocha-Filho, Formation and stability of oil-in-water nanoemulsions containing rice bran oil: in vitro and in vivo assessments, *J. Nanobiotechnol.* 9 (2011) 44, <https://doi.org/10.1186/1477-3155-9-44>.
- [56] N.P. Nirmal, R. Meredyd, L. Li, Y. Sultanbawa, Formulation, characterisation and antibacterial activity of lemon myrtle and anise myrtle essential oil in water nanoemulsion, *Food Chem.* 254 (2019) 1–7, <https://doi.org/10.1016/j.foodchem.2018.01.173>.
- [57] S.M. Jafari, Y. He, B. Bhandari, Nano-emulsion production by sonication and microfluidization – a comparison, *Int. J. Food Prop.* 9 (2006) 475–485, <https://doi.org/10.1080/10942910600596464>.
- [58] C. Agarwal, K. Mátéh, T. Hofmann, L. Csóka, Ultrasound-assisted extraction of cannabinoids from *Cannabis sativa* L. optimized by response surface methodology, *J. Food Sci.* 83 (2018) 700–710, <https://doi.org/10.1111/1750-3841.14075>.
- [59] A. Azeem, M. Rizwan, F.J. Ahmad, Z. Iqbal, R.K. Khar, M. Aqil, S. Talegaonkar, Nanoemulsion components screening and selection: a technical note, *AAPS PharmSciTech* 10 (2009) 69–76, <https://doi.org/10.1208/s12249-008-9178-x>.
- [60] D.J. McClements, J. Rao, Food-grade nanoemulsions: formulation, fabrication, properties, performance, biological fate, and potential toxicity, *Crit. Rev. Food Sci. Nutr.* 51 (2011) 285–330, <https://doi.org/10.1080/10408398.2011.559558>.
- [61] J. Xue, Essential Oil Nanoemulsions Prepared with Natural Emulsifiers for Improved Food Safety. (Ph.D. thesis), University of Tennessee, 2015.
- [62] D. Paolino, C.A. Ventura, S. Nisticò, G. Puglisi, M. Fresta, Lecithin microemulsions for the topical administration of ketoprofen: percutaneous adsorption through human skin and in vivo human skin tolerability, *Int. J. Pharm.* 244 (2002) 21–31, [https://doi.org/10.1016/S0378-5173\(02\)00295-8](https://doi.org/10.1016/S0378-5173(02)00295-8).
- [63] U. Etcheberria, A.L. de la Garza, J. Campión, J.A. Martínez, F.I. Milagro, Antidiabetic effects of natural plant extracts via inhibition of carbohydrate hydrolysis enzymes with emphasis on pancreatic alpha amylase, *Expert Opin. Ther. Targets* 16 (2012) 269–297, <https://doi.org/10.1517/14728222.2012.664134>.
- [64] F.M. Ashcroft, D.E. Harrison, S.J. Ashcroft, Glucose induces closure of single potassium channels in isolated rat pancreatic beta-cells, *Nature* 312 (1984) 446–448, <https://doi.org/10.1038/312446a0>.
- [65] D.L. Cook, C.N. Hales, Intracellular ATP directly blocks K⁺ channels in pancreatic B-cells, *Nature* 311 (1984) 271–273, <https://doi.org/10.1038/311271a0>.
- [66] J.C. Henquin, Triggering and amplifying pathways of regulation of insulin secretion by glucose, *Diabetes* 49 (2000) 1751–1760, <https://doi.org/10.2337/diabetes.49.11.1751>.
- [67] Z. Iqbal, G. Morahan, M. Arooj, A.N. Sobolev, S. Hameed, Synthesis of new arylsulfonylspiroimidazolidine-2',4'-diones and study of their effect on stimulation of insulin release from MIN6 cell line, inhibition of human aldose reductase, sorbitol accumulations in various tissues and oxidative stress, *Eur. J. Med. Chem.* 168 (2019) 154–175, <https://doi.org/10.1016/j.ejmech.2019.02.036>.
- [68] R.P. Kelly, R. Sutton, F.M. Ashcroft, Voltage-activated calcium and potassium currents in human pancreatic beta-cells, *J. Physiol.* 443 (1991) 175–192, <https://doi.org/10.1113/jphysiol.1991.sp018829>.
- [69] J.C. Henquin, Regulation of insulin secretion: a matter of phase control and amplitude modulation, *Diabetologia* 52 (2009) 739–751, <https://doi.org/10.1007/s00125-009-1314-y>.
- [70] A.R. Saltiel, C.R. Kahn, Insulin signaling and the regulation of glucose and lipid metabolism, *Nature* 414 (2001) 799–806, <https://doi.org/10.1038/414799a>.
- [71] R.A. DeFronzo, R.C. Bonadonna, E. Ferrannini, Pathogenesis of NIDDM. A balanced overview, *Diabetes Care* 15 (1992) 318–368, <https://doi.org/10.2337/diacare.15.3.318>.
- [72] R.T. Watson, J.E. Pessin, Bridging the GAP between insulin signaling and GLUT4 translocation, *Trends Biochem. Sci.* 31 (2006) 215–222, <https://doi.org/10.1016/j.tibs.2006.02.007>.
- [73] K.F. Petersen, G.I. Shulman, Etiology of insulin resistance, *Am. J. Med.* 119 (2006) S10–S16, <https://doi.org/10.1016/j.amjmed.2006.01.009>.
- [74] S. Pandeti, D. Arha, A. Mishra, S.S. Reddy, A.K. Srivastava, T. Narendra, A. K. Tamrakar, Glucose uptake stimulatory potential and antidiabetic activity of the Arnebin-1 from *Arnebia nobilis*, *Eur. J. Pharmacol.* 789 (2016) 449–457, <https://doi.org/10.1016/j.ejphar.2016.08.010>.
- [75] T. Szkudelski, The mechanism of alloxan and streptozotocin action in B cells of the rat pancreas, *Physiol. Res.* 50 (2001) 537–546.
- [76] S. Gheibi, K. Kashfi, A. Ghasemi, A practical guide for induction of type-2 diabetes in rat: incorporating a high-fat diet and STZ, *Biomed. Pharmacother.* 95 (2017) 605–613, <https://doi.org/10.1016/j.biopharm.2017.08.098>.
- [77] A. Mahalakshmi, G.A. Kurian, Evaluating the impact of diabetes and diabetic cardiomyopathy rat heart on the outcome of ischemia-reperfusion associated oxidative stress, *Free Radic. Biol. Med.* 118 (2018) 35–43, <https://doi.org/10.1016/j.freeradbiomed.2018.02.021>.
- [78] Y. Sheng, S. Zheng, T. Ma, C. Zhang, X. Ou, X. He, W. Xu, K. Huang, Mulberry leaf alleviates STZ-induced diabetic rats by attenuating NEFA signaling and modulating intestinal microflora, *Sci. Rep.* 7 (2017) 12041, <https://doi.org/10.1038/s41598-017-12245-2>.
- [79] J. Naowaboot, P. Pannangpetch, V. Kukongviriyapan, U. Kukongviriyapan, S. Nakmareong, A. Itharat, Mulberry leaf extract restores arterial pressure in

- streptozotocin-induced chronic diabetic rats, Nutr. Res. 29 (2009) 602–608, <https://doi.org/10.1016/j.nutres.2009.06.002>.
- [80] V.P. Choudhari, K.P. Gore, A.T. Pawar, Antidiabetic, antihyperlipidemic activities and herb-drug interaction of a polyherbal formulation in streptozotocin induced diabetic rats, J. Ayurveda Integr. Med. 8 (2017) 218–225, <https://doi.org/10.1016/j.jaim.2016.11.002>.
- [81] X. Tang, O.J. Olatunji, Y. Zhou, X. Hou, *Allium tuberosum*: Antidiabetic and hepatoprotective activities, Food Res. Int. 102 (2017) 681–689, <https://doi.org/10.1016/j.foodres.2017.08.034>.
- [82] B.V. Howard, D.C. Robbins, M.L. Sievers, E.T. Lee, D. Rhoades, R.B. Devereux, W. J. Howard, LDL cholesterol as a strong predictor of coronary heart disease in diabetic individuals with insulin resistance and low LDL: the strong heart study, Arterioscler. Thromb. Vasc. Biol. 20 (2000) 830–835, <https://doi.org/10.1161/01.ATV.20.3.830>.
- [83] B.M. Moukette, V.J. Ama Moor, C.P. Biapa Nya, P. Nanfack, F.T. Nzufu, M. A. Kenfack, J.Y. Ngogang, C.A. Pieme, Antioxidant and synergistic antidiabetic activities of a three-plant preparation used in Cameroon folk medicine, Int. Sch. Res. Not. 2017 (2017), 9501675, <https://doi.org/10.1155/2017/9501675>.
- [84] N. Vargas-Mendoza, E. Madrigal-Santillan, A. Morales-Gonzalez, J. Esquivel-Soto, C. Esquivel-Chirino, M.G.L.Y. González-Rubio, J.A. Gayosso-de-Lucio, J. A. Morales-González, Hepatoprotective effect of silymarin, World J. Hepatol. 6 (2014) 144–149, <https://doi.org/10.4254/wjh.v6.i3.144>.
- [85] S.B. Sharma, A. Nasir, K.M. Prabhu, P.S. Murthy, Antihyperglycemic effect of the fruit-pulp of *Eugenia jambolana* in experimental diabetes mellitus, J. Ethnopharmacol. 104 (2006) 367–373, <https://doi.org/10.1016/j.jep.2005.10.033>.
- [86] T.A. More, B.R. Kulkarni, M.L. Nalawade, A.U. Arvindekar, Antidiabetic activity of linalool and limonene in streptozotocin-induced diabetic rat: a combinatorial therapy approach, Int. J. Pharm. Pharm. Sci. 6 (8) (2014) 159–163.
- [87] S. Rani, S. Sharma, S. Kumar, To investigate antihyperglycemic and antihyperlipidemic potential of safrole in rodents by in-vivo and in-vitro study, Drug Res. 64 (6) (2014) 287–295, <https://doi.org/10.1055/s-0033-1357192>. (<http://doi.org/>).